The formulation of a chloroquinoline derivative in an amorphous solid dispersion for improved solubility

N Raghunandan

orcid.org/ 0000-0002-5028-4158

Dissertation accepted in fulfilment of the requirements for the degree Master of Science in Pharmaceutical Sciences at the North-West University

Supervisor: Dr T Moodley

Co-Supervisor: Prof W Liebenberg

Graduation: May 2026

TABLE OF CONTENTS

LIST OF ABBREVIATIONS

ΔG - Gibbs free energy

ASDs - Amorphous solid dispersions

APIs - Active pharmaceutical ingredients

BCS - Biopharmaceutical classification system

CBU - Chloroquinoline urea benzothiazole derivative

DCM - Dichloromethane

DMSO - Dimethyl sulfoxide

DSC - Differential scanning calorimetry

FT-IR - Fourier transform infrared spectroscopy

FWHM - Full Width at Half Maximum

GI - Gastrointestinal

HCl - Hydrochloric acid

HME - Hot melt extrusion

HPMC - Hydroxypropyl methylcellulose

HPMC-AS - Hydroxypropyl methylcellulose acetate succinate

ICH - International Council for Harmonisation of Technical Requirements for Pharmaceuticals for Human Use

mDSC - Modulated differential scanning calorimetry

n.d - No date

NMR - Nuclear magnetic resonance

PDF - Pair distribution function

PEG - Polyethylene glycol

PLM - Polarised light microscopy

PVP - Polyvinylpyrrolidone

PVP/VA - Polyvinylpyrrolidone vinyl acetate

RM - Raw material

STA - Simultaneous thermal analysis

*T*g - Glass transition temperature

TGA - Thermogravimetric analysis

*T*m - Melting temperature

USP - United States Pharmacopeia

UV – Ultraviolet

VA- Vinyl acetate

XRPD - X-ray powder diffraction

LIST OF FIGURES

LIST OF TABLES

ACKNOWLEDGEMENTS

This dissertation marks the culmination of a long and challenging journey—one that would not have been possible without the support, encouragement, and guidance of many remarkable individuals and institutions.

First and foremost, I would like to express my deepest gratitude to my supervisors, Prof. Wilna Liebenberg and Dr. Thrineshen Moodley, whose unwavering mentorship, critical insight, and constant encouragement made this work possible. Their guidance not only shaped the direction of this project but also nurtured my growth as a pharmaceutical scientist and my career as a pharmacist as a whole.

To the NWU Preclinical Drug Development Platform (PCDDP), thank you for granting me the opportunity to pursue this research and for providing a world-class environment in which to learn and grow. I am especially thankful to PharmaCen for embracing me as one of their own for adopting me into their student family, and for being a steady source of strength and solidarity when the weight of the Master's journey felt overwhelming. Your support carried me.

A special thanks to Dr. Righard Lemmer, whose infectious passion for pharmaceutics and countless stimulating conversations on amorphous solid dispersions kept me inspired. To Madelain, thank you for your patience, precision and positivity during the UV/Vis work and for always having so many amazing stories to tell during the arduous hours of work. You were a critical part of this project's success.

To my family: my dad, whose quiet strength gave me courage; my sister, whose belief in me never wavered; and to my mum, whose love still lives in every part of me despite her absence. I also dedicate this work to my best friend, who is no longer with us but whose shining example as an academic, a pharmacist and a confidant will always be carried with me wherever life takes me.

This journey was not walked alone. Each of you made this possible. From the depths of my heart, thank you.

ABSTRACT

Poor aqueous solubility remains a major hurdle in the development of orally administered drugs, particularly those with promising pharmacological activity but limited bioavailability. This study addresses this issue through the formulation of an amorphous solid dispersion (ASD) containing a novel chloroquinoline derivative composed of chloroquinoline, urea, and benzothiazole moieties. The objective was to enhance the solubility and dissolution rate of this poorly soluble compound using polyvinylpyrrolidone (PVP K25) as a hydrophilic polymer carrier.

The ASD was prepared via solvent evaporation, and a 1:4 drug-to-polymer ratio was identified as optimal based on preliminary miscibility and thermal analyses. Comprehensive physicochemical characterization was conducted using differential scanning calorimetry (DSC), modulated DSC (MDSC), X-ray powder diffraction (XRPD), thermogravimetric analysis (TGA), Fourier-transform infrared spectroscopy (FTIR), and polarised light microscopy (PLM). Thermal data confirmed the amorphous nature of the dispersion, with the disappearance of the crystalline drug melting peak and a single glass transition temperature (*T*g), indicative of miscibility. XRPD and PLM further supported the loss of crystallinity in the ASD formulation.

Solubility studies demonstrated a significant increase in aqueous solubility for the ASD compared to the raw material, and UV-Vis validated dissolution tests showed faster and more complete drug release in both water and acidic media. These findings confirm that the ASD strategy substantially improves the dissolution properties of the chloroquinoline derivative, laying the groundwork for further preclinical development.

Keywords: amorphous solid dispersion (ASD), chloroquinoline derivative, solubility enhancement, PVP K25, glass transition temperature (*T*g), X-ray powder diffraction (XRPD), dissolution, poorly soluble drugs, pharmaceutical formulation, differential scanning calorimetry (DSC).

CHAPTER 1

Introduction

1.1 Background information

A chloroquinoline derivative represented in Figure 1.1 is a hybrid molecule that combines the therapeutic attributes of chloroquinoline, urea, and benzothiazole pharmacophores. Hybrid molecules offer the potential to synergistically enhance the pharmacological benefits of its component pharmacophores into a singular entity with superior medicinal efficacy (Kumar et al*.,* 2020; Singh et al., 2022; H. Singh & Agrawal, 2022). Figure 1.2 depicts the synthetic route used to produce the chloroquinoline derivative. The activated chloro group on the quinoline was replaced with $H_2N–(CH_2CH_2NH)_n–H$ (n = 0–6) to give amino-spacer intermediates. The primary amine was then coupled with a benzothiazole isocyanate to form the urea, affording the quinoline–urea–benzothiazole products (Moodley et al., 2022).

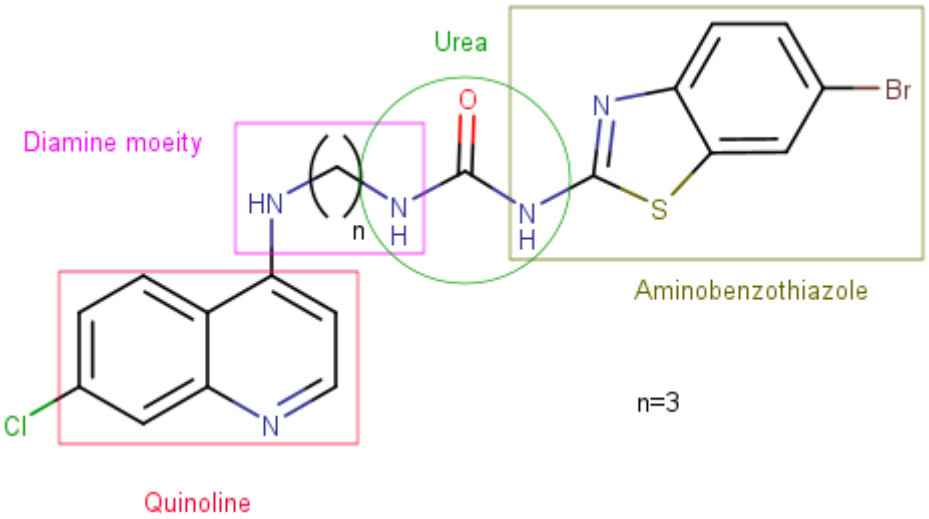

Figure 1.1: The chloroquinoline derivative containing chloroquinoline, urea and an aminobenzothiazole moiety.

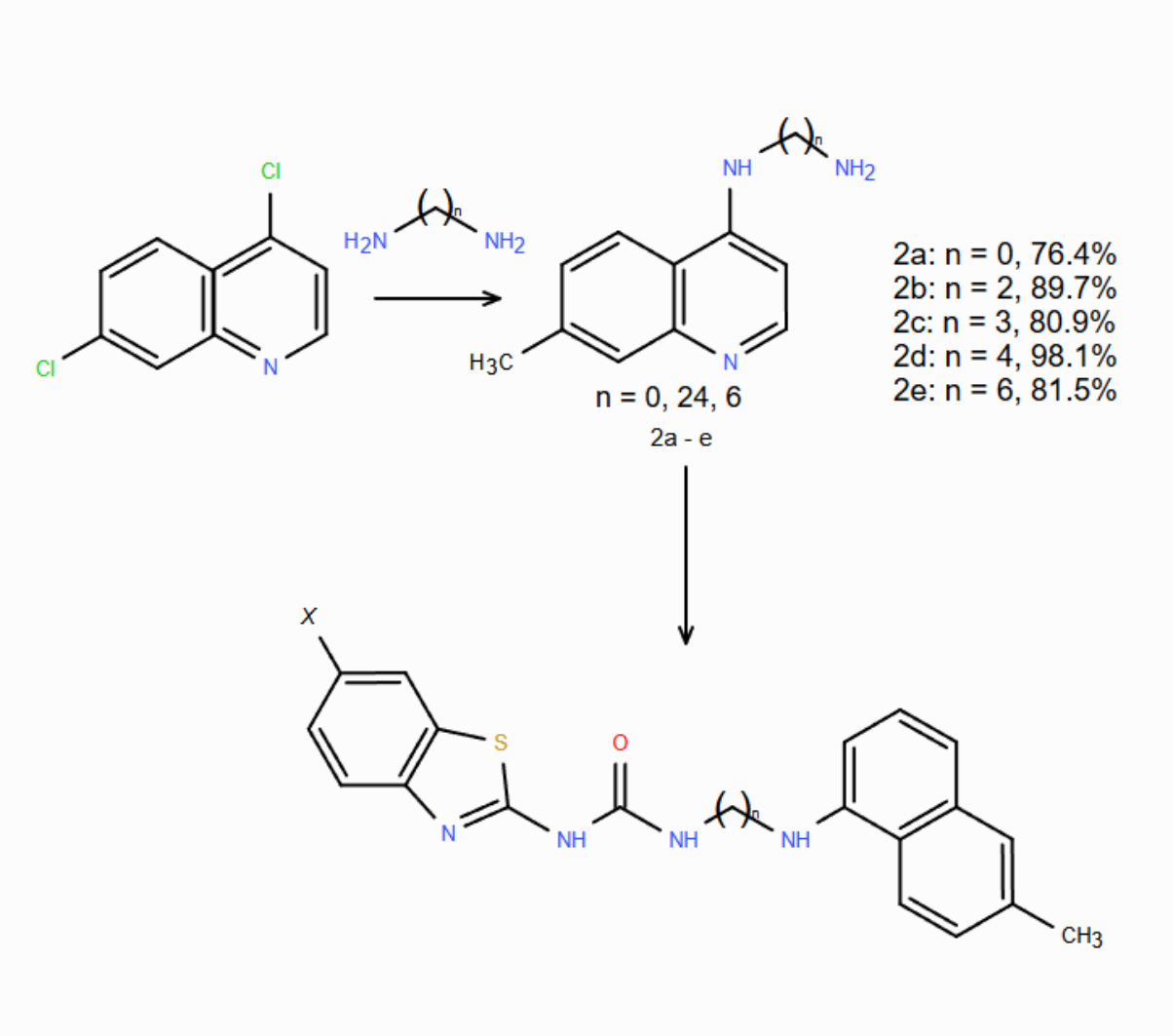

Figure 1.2: Synthetic route of the chloroquinoline derivative (adapted from Moodley et al., 2022).

The chloroquinoline derivative exhibits promising antimicrobial, antimalarial and potency characteristics akin to those of Biopharmaceutical classification system (BCS) class II or IV drugs — which are marked by low solubility combined with either high or low intestinal permeability respectively (Islam et al., 2024; Papich & Martinez, 2015). Therefore, this compound has emerged as a prime candidate for formulation research focused on elevating its solubility and dissolution.

This study aims to develop an amorphous solid dispersion (ASD) formulation for the chloroquinoline derivative.

Research has consistently shown that ASDs can significantly enhance the bioavailability of drugs with low solubility (Correa-Soto et al., 2022; Iyer et al., 2021; Pandi et al., 2020). For instance, two specific ASD formulations of the antifungal agent itraconazole, showed an increased bioavailability *in vivo* compared to its commercially available crystalline counterpart,

Sporanox® (Feng et al., 2018). Additionally, an ASD of the anti-inflammatory medication celecoxib exhibited a marked improvement in oral bioavailability relative to its crystalline version (Meng et al., 2019; Motallae et al., 2018; Pöstges et al., 2022; Schittny et al., 2020; Tambe et al., 2022).

1.2 Research Problem

Poor aqueous solubility of novel compounds produced in the lead optimisation stages of the drug delivery pipeline critically limits its bioavailability *in vivo* and, thus, its effectiveness as a therapeutic agent. Therefore, there is a need to investigate formulation strategies to further explore the potential of enhancing a compound's solubility *in vitro* before it is tested in *in vivo* systems.

1.2.1 AIM AND OBJECTIVES

1.2.1.1 Aim

The chloroquinoline derivative's formulation with an ASD prepared by solvent evaporation will be investigated by characterisation techniques such as Differential Scanning Calorimetry (DSC), Modulated Differential Scanning Calorimetry (mDSC), Fourier Transform Infrared Spectroscopy (FT-IR), X-ray Powder Diffraction (XRPD) and Polarised Light Microscopy (PLM). These techniques will provide valuable thermal, structural and morphological information about the formulation. *In vitro* solubility and dissolution studies will then proceed in simulated media.

1.2.1.2 Objectives

- The development and optimisation of an amorphous solid dispersion (ASD) drug/polymer formulation. This will involve screening a drug/polymer combination using DSC, mDSC, XRPD and PLM to evaluate the amorphous structure of the dispersion.
- The method development and validation of a UV spectroscopy method to quantitatively determine the concentration of the chloroquinoline derivative during solubility and dissolution testing.
- To conduct *in vitro* solubility and dissolution studies using USP apparatus II and quantitatively analyse the raw compound vs ASD.

1.3 Study Design

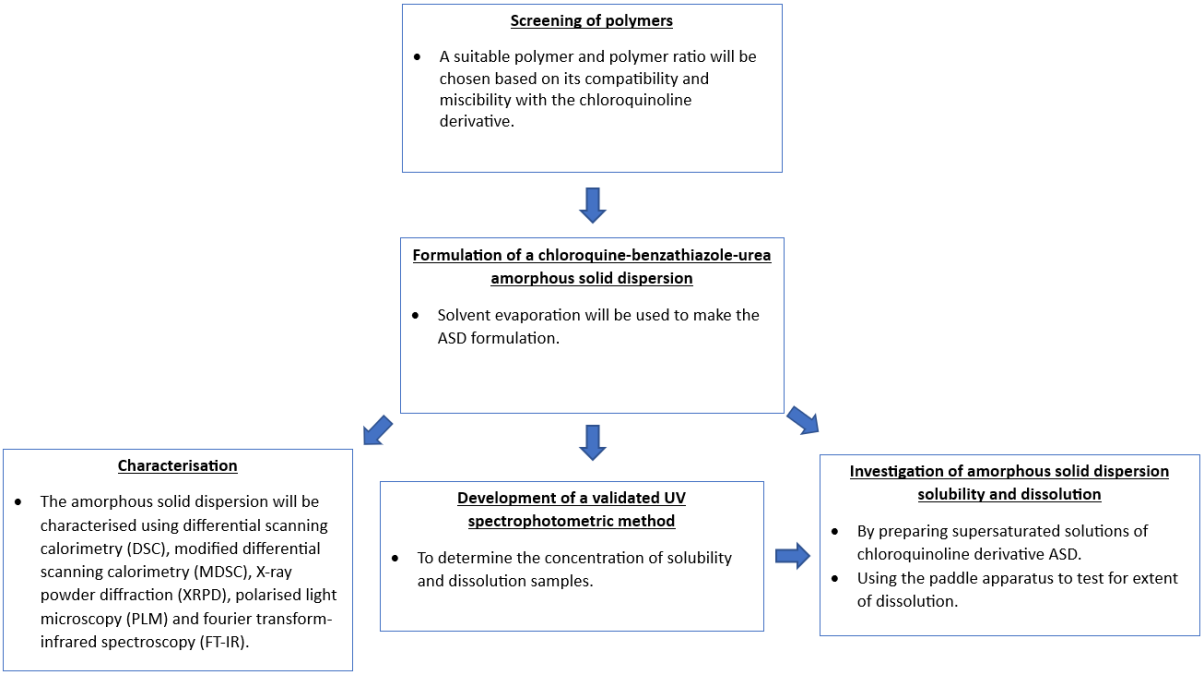

Figure 1.3: A flow diagram depicting the 5 phases of a chloroquinoline derivative ASD formulation, characterisation and dissolution.

1.4 Ethical considerations

This study was approved by the NWU AnimCare Research Ethics Committee (NWU 02013-23-S5).

No live animals will be used during the research. Therefore, consideration must be taken regarding research confidentiality and honest results communication. Any information used, communicated, or conveyed surrounding the study will be given or reported in an honest manner, without plagiarism of any form, therefore, ensuring that the research done is original and trustworthy. Research findings will be discussed with the highest possible level of objectivity. Any individuals involved or who have contributed in any way, shape, or form to the research will be acknowledged in both name and role. Immoral research practices or research misconduct of any kind will be reported to the relevant authorities. The study will follow the process for a category 0 application to the North-West University Animal Care, Health and Safety Research Ethics Committee (NWU-AnimCareREC). All the processes used during the study will follow the principles of the 12Rs (replacement, reduction, refinement, responsibility, relevance, reproducibility, respect, reporting, review, responsiveness, rescue, reflection) (Brink & Lewis, 2023).

1.5 Dissertation overview

Chapter 1: This chapter provides an overview of the rationale and research methods to be used in this study.

Chapter 2: A comprehensive literature review will delve into the intricacies of the solid-state characteristics and complexities of ASDs and its role in the overall improvement in the bioavailability of active pharmaceutical ingredients.

Chapter 3: The results obtained from the study will be presented in a paper format.

Chapter 4: This will provide a conclusion of the study where the results obtained will be summarised and recommendations will be given for future studies.

Reference list

Brink, C. B., & Lewis, D. I. (2023). The 12 Rs Framework as a Comprehensive, Unifying Construct for Principles Guiding Animal Research Ethics. *Animals*, 13(7), 1128. https://doi.org/10.3390/ani13071128

Correa-Soto, C. E., Gao, Y., Indulkar, A. S., Zhang, G. G. Z., & Taylor, L. S. (2022). Role of surfactants in improving release from higher drug loading amorphous solid dispersions. *International Journal of Pharmaceutics*, 625, 122120. https://doi.org/10.1016/j.ijpharm.2022.122120

Feng, D., Peng, T., Huang, Z., Singh, V., Shi, Y., Wen, T., Lu, M., Quan, G., Pan, X., & Wu, C. (2018). Polymer–surfactant system-based amorphous solid dispersion: Precipitation inhibition and bioavailability enhancement of itraconazole. *Pharmaceutics*, 10(2), 53. https://doi.org/10.3390/pharmaceutics10020053

Iyer, R., Jovanovska, V. P., Berginc, K., Jaklič, M., Fabiani, F., Harlacher, C., Huzjak, T., & Sanchez-Felix, M. V. (2021). Amorphous solid dispersions (ASDs): The influence of material properties, manufacturing processes and analytical technologies in drug product development. *Pharmaceutics*, 13(10), 1682. https://doi.org/10.3390/pharmaceutics13101682

Islam, S., Shahzad, S. A., Ismail, T., Sherani, U. A. S., Khan, K. M., Fatima, N., Khan, S. A., & Mannan, A. (2024). Exploring the antimicrobial and cytotoxic potential of novel chloroquine analogues. *Future Medicinal Chemistry*, 16(8), 737–750. https://doi.org/10.4155/fmc-2023-0343

Meng, F., Ferreira, R., & Zhang, F. (2019). Effect of surfactant level on properties of celecoxib amorphous solid dispersions. *Journal of Drug Delivery Science and Technology*, 49, 301–307. https://doi.org/10.1016/j.jddst.2018.11.026

Moodley, R., Mashaba, C., Rakodi, G. H., Ncube, N. B., Maphoru, M. V., Balogun, M. O., Jordan, A., Warner, D. F., Khan, R., & Tukulula, M. (2022). New quinoline–urea–benzothiazole hybrids as promising antitubercular agents: Synthesis, in vitro antitubercular activity, cytotoxicity studies, and in silico ADME profiling. Pharmaceuticals, 15(5), 576. https://doi.org/10.3390/ph15050576

Motallae, S., Taheri, A., & Homayouni, A. (2018). Preparation and characterization of solid dispersions of celecoxib obtained by spray-drying ethanolic suspensions containing PVP-K30 or isomalt. *Journal of Drug Delivery Science and Technology*, 46, 188–196. https://doi.org/10.1016/j.jddst.2018.05.020

Pandi, P., Bulusu, R., Kommineni, N., Khan, W., & Singh, M. (2020). Amorphous solid dispersions: An update for preparation, characterization, mechanism on bioavailability, stability, regulatory considerations and marketed products*. International Journal of Pharmaceutics,* 586, 119560. https://doi.org/10.1016/j.ijpharm.2020.119560

Papich, M. G., & Martinez, M. N. (2015). Applying Biopharmaceutical Classification System (BCS) criteria to predict oral absorption of drugs in dogs: Challenges and pitfalls. *AAPS Journal,* 17(4), 948–964. https://doi.org/10.1208/s12248-015-9743-7

Pöstges, F., Kayser, K., Stoyanov, E., & Wagner, K. G. (2022). Boost of solubility and supersaturation of celecoxib via synergistic interactions of methacrylic acid-ethyl acrylate copolymer (1:1) and hydroxypropyl cellulose in ternary amorphous solid dispersions. *International Journal of Pharmaceutics*: X, 4, 100115. https://doi.org/10.1016/j.ijpx.2022.100115

Sampath Kumar, H. M., Herrmann, L., & Tsogoeva, S. B. (2020). Structural hybridization as a facile approach to new drug candidates*. Bioorganic & Medicinal Chemistry Letters*, 30(23), 127514. https://doi.org/10.1016/j.bmcl.2020.127514

Schittny, A., Huwyler, J., & Puchkov, M. (2020). Mechanisms of increased bioavailability through amorphous solid dispersions: A review. *Drug Delivery,* 27(1), 110–127. https://doi.org/10.1080/10717544.2019.1704940

Singh, A. K., Kumar, A., Singh, H., Sonawane, P., Paliwal, H., Thareja, S., Pathak, P., Grishina, M., Jaremko, M., Emwas, A. H., Yadav, J. P., Verma, A., Khalilullah, H., & Kumar, P. (2022). Concept of hybrid drugs and recent advancements in anticancer hybrids. *Pharmaceuticals*, 15(9), 1071. https://doi.org/10.3390/ph15091071

Singh, H., & Agrawal, D. K. (2022). Recent advances in the development of active hybrid molecules in the treatment of cardiovascular diseases. *Bioorganic & Medicinal Chemistry*, 62, 116706. https://doi.org/10.1016/j.bmc.2022.116706

Tambe, S., Jain, D., Meruva, S. K., Rongala, G., Juluri, A., Nihalani, G., Mamidi, H. K., Nukala, P. K., & Bolla, P. K. (2022). Recent advances in amorphous solid dispersions: Preformulation, formulation strategies, technological advancements and characterization. *Pharmaceutics*, 14(10), 2203. https://doi.org/10.3390/pharmaceutics14102203

CHAPTER 2

Literature Review

This chapter provides an overview of analytical techniques, experiments, parameters and systems that have the potential to be used in the investigation of an ASD formulated chloroquinoline derivative.

2.1 Biopharmaceutical classification systems of APIs

The Biopharmaceutical Classification System provides insight into the oral solubility and permeability of an API *in vivo* (Dahan et al., 2009; Papich & Martinez, 2015). It is composed of four broad categories which can be seen in Figure 2.1.

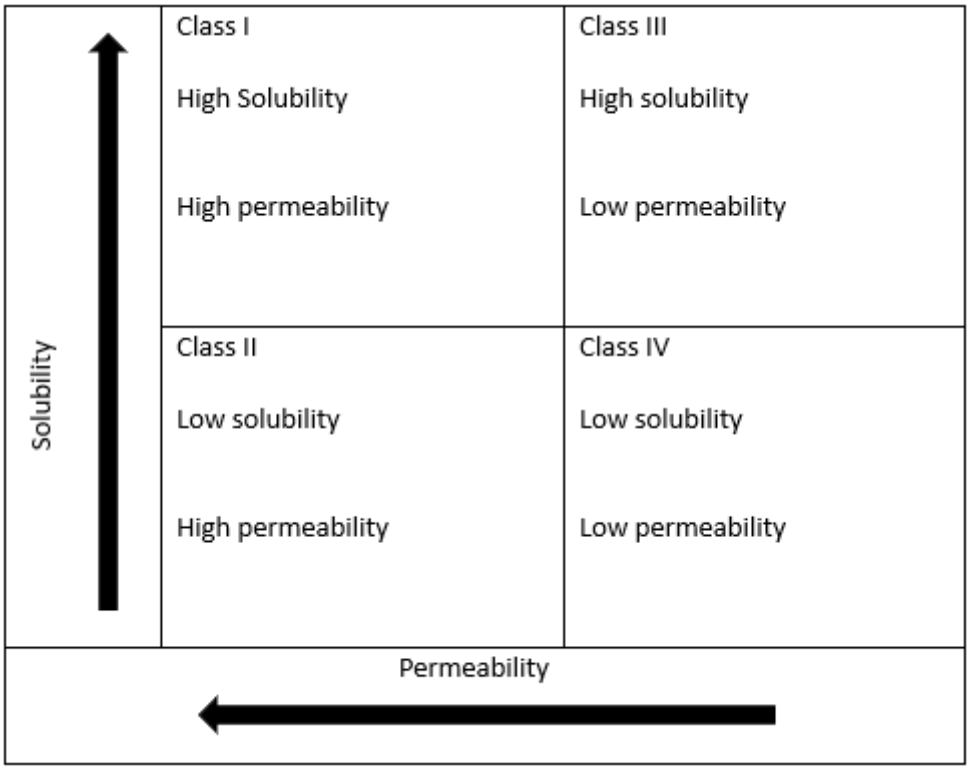

Figure 2.1: The Biopharmaceutics Classification System (Dahan et al. 2009).

This system illustrates that class I drugs are considered to have ideal solubility and membrane permeability characteristics. Class II drugs generally have poor solubility and high membrane permeability, this is the opposite for class III and class IV compounds and therefore there is a need to formulate these classes of APIs for improved drug delivery (Dahan et al., 2009; Papich & Martinez, 2015; Samineni et al., 2022).

This was found with furosemide, a diuretic medication classified under BCS Class IV. Reduction of particle size and increasing surface area through the use of nanosuspensions

achieved supersaturation states and enhanced dissolution rates in the gastrointestinal environment (Gulsun et al., 2018).

Improved solubility and dissolution were also seen with BCS Class IV drug, hydrochlorothiazide, which was formulated with cyclodextrin, formulations that take advantage of an amphiphilic structure to encapsulate hydrophobic drug molecules and facilitate solubilisation (Maestrelli et al., 2020; Mendes et al., 2016; Pires et al., 2011).

Some APIs show crystalline properties which are thermodynamically stable due to their ordered molecular structure thus effecting their overall solubility properties *in vivo* (Healy et al., 2017; Jones et al., 2014). Amorphous solids lack long-range molecular order and are characterised by randomly arranged molecules and are therefore used in the formulation of BCS class II and IV drugs since they lead to increased solubility and dissolution (Liu et al., 2021; Shi et al., 2020, Jones & Bimbo, 2020).

2.2. Amorphous Solid Dispersions

Amorphous solid dispersions (ASDs) consist of an API dispersed in a polymer matrix at a molecular level, forming a single-phase amorphous entity where all components are dispersed homogeneously without any phase separation and generally depict a disorganised structure compared to crystalline materials as shown in Figure 2.2 (Pandi et al., 2020; Shi et al., 2022).

Yun et al. (2024) demonstrated that carefully chosen polymers, such as HPMC, can maintain the amorphous state of a low-solubility anticancer drug and prevent recrystallization. By employing spray drying, they achieved a homogeneous drug–polymer mixture that significantly boosted dissolution and oral bioavailability. Their findings highlight the importance of polymer selection and process optimization in creating robust amorphous solid dispersions for challenging APIs.

A recent study by Patel et al. (2023) showcased how hot-melt extrusion can effectively disperse a poorly soluble drug within a thermoplastic carrier, leading to enhanced solubility and faster release. This method leverages elevated processing temperatures to form a stable amorphous matrix, with minimal solvent usage and good scalability. The authors emphasized that polymer compatibility and extrusion parameters are important in achieving uniform dispersions and sustained supersaturation, characteristics that are hallmark features of typical ASDs.

Newman et al. (2020) emphasised this by combining the API with a suitable polymer, the resultant ASD is more stable than the amorphous API alone due to the polymer’s ability to interfere with the crystallisation process (Shi et al., 2020).

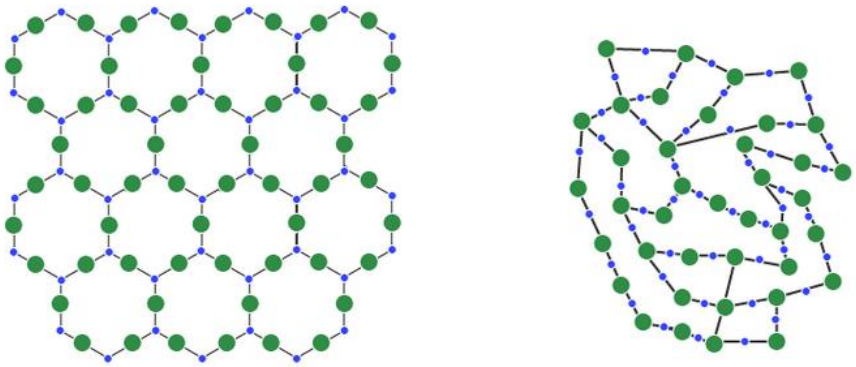

Crystalline state Amorphous state

Figure 2.2: Showing structural differences between crystalline and amorphous states (adapted from Einfalt et al., 2013).

While the amorphous state itself generally leads to improved solubility, numerous studies have provided structured examples demonstrating how specific ASDs can markedly enhance dissolution. Indomethacin was formulated as an ASD with polymers like PVP and HPMC-AS, resulting in significantly higher dissolution rates compared to its crystalline counterpart (Andrews et al., 2023; Sun et al., 2012). Similarly, celecoxib, another poorly soluble API, showed supersaturation leading to improved dissolution profiles and increased bioavailability when formulated into ASDs with HPMC or polyvinylpyrrolidone vinyl acetate (PVP/VA), (Andrews et al., 2023; Figueiredo et al., 2024; Holm et al., 2022). In another study, carvedilol, a beta-blocker with low aqueous solubility, had been successfully formulated as an ASD via solvent method with PVP/VA copolymer (Krstić et al., 2020). Additionally, aprepitant, a neurokinin-1 receptor antagonist used to prevent chemotherapy-induced nausea, has also benefited from ASD formulation. The drug was also dispersed uniformly within a polymer matrix using solvent evaporation method, researchers achieved a significant increase in its dissolution rate and a prolonged supersaturated state in gastrointestinal fluids. This approach has shown potential to result in enhanced *in vivo* absorption and therefore improved therapeutic performance (Liu et al., 2022).

Recent studies have focused on improving the understanding of drug-polymer interactions at the molecular level to better predict and enhance the stability of ASDs. Central to these developments is the understanding that hydrogen bonding, hydrophobic interactions, and antiplasticisation govern drug-polymer miscibility and inhibit crystallisation. For instance, hydrogen bonding between functional groups in polymers like HPMC-AS and drugs such as

itraconazole has been shown to reduce molecular mobility, thereby stabilising the amorphous state (Zhang et al., 2023). Similarly, hydrophobic interactions between polymers (e.g., Soluplus®) and hydrophobic drugs (e.g., celecoxib) promote micelle-like structures that sustain supersaturation and facilitate effective dissolution (Patel et al., 2022). Advanced characterization techniques, including molecular dynamics simulations and solid-state NMR, have enabled precise mapping of these interactions, revealing how polymers like PVP act as antiplasticisers by elevating the *T*g of low *T*g drugs such as ritonavir (Bohg et al., 2021; Melnyk et al., 2017). Pair distribution function (PDF) analysis further elucidates nanoscale structural heterogeneity, linking phase separation to instability risks (Billinge, 2019). Predictive modelling approaches, such as Flory-Huggins theory and machine learning, now complement experimental methods, enabling rational polymer selection based on solubility parameters and large datasets (Nistane et al., 2022; Zhu et al., 2025). Despite progress, challenges persist, including hygroscopicity-driven destabilisation and the complexity of ternary systems, necessitating innovations in polymer engineering (Jacob et al., 2025).

Collectively, these molecular insights are transforming ASD design, shifting the paradigm from empirical trial-and-error to mechanism-driven formulation strategies, with profound implications for bioavailability enhancement and commercial scalability (Chiang et al., 2023).

2.3 Formulation Strategies of ASDs

Physical mixing or dry blending of an API with a polymer can be considered an early formulation strategy offering limited improvement in solubility and dissolution profiles. This was seen with fenofibrate, a poorly soluble API, which was physically mixed with a hydrophilic polymer hydroxypropyl cellulose, resulting in a partially crystalline formulation, ultimately providing only modest solubility enhancements from this incomplete amorphisation (Martin-Pastor & Stoyanov, 2021; Reppas et al., 2023).

Hot melt extrusion (HME) involves the formulation of an ASD via a process where the drug and polymer are blended and heated above the polymer's *T*g, then forced through a screw extruder where thermal energy and mechanical shear promote molecular dispersion (Patil et al., 2016). This formulation strategy produces more uniform dispersions than simple blending (Simões et al., 2019). In the case of celecoxib ASDs prepared by HME with cellulose-based polymers, an improved physical stability was found when compared to their physical mixtures amongst an improvement of other predicted qualities such as solubility (Holm et al., 2022; Pöstges et al., 2022; Zhang et al., 2023).

Another formulation strategy is spray drying which allows for rapid solvent removal through atomisation of the liquid feed into droplets therefore maximising surface area for instantaneous

convective heat transfer and controlled particle formation. Studies with ritonavir, an antiretroviral drug known for its poor aqueous solubility demonstrated that spray drying could produce stable amorphous systems with enhanced dissolution profiles compared to earlier methods such as physical mixing or HME (Fayed et al., 2022; Hamed et al., 2021; Nguyen & Van Den Mooter, 2014).

Solvent evaporation methods (e.g., rotary evaporation, vacuum drying) have a core focus of controlled particle formation. These methods are carried out at milder temperatures than HME and with a more straightforward process control than spray drying. Atorvastatin-ASDs have been prepared by solvent evaporation to achieve a homogeneously amorphous matrix with a clearly defined *T*g, which is a reversible change of a material from a hard glassy state to a soft rubbery state, and improved dissolution rates relative to its crystalline form from earlier, less refined approaches thus demonstrating the evolution and elaborateness of ASD preparation techniques over time (Kim et al*.,* 2013; Kwon et al., 2019; Shamsuddin et al*.*, 2016). By fine-tuning the solvent composition, drying conditions, and drug-polymer ratio, solvent evaporation can yield ASDs that are both robust and scalable.

2.4 Glass Transition Temperature (*T*g) and its Significance in Amorphous Solids

The *T*g is indicative of the point at which molecular mobility is significantly reduced and is influenced by the composition and thermal characteristics of the material. When a molten drug is cooled quickly, it can bypass the crystallisation process and form an amorphous state. This supercooled liquid stays in equilibrium with the molten drug below its melting temperature (*T*m) until it reaches the *T*g (Debenedetti & Stillinger, 2001; Iyer et al*.*, 2021). At *T*g, the material solidifies into an amorphous state and falls out of equilibrium. Our aim is to achieve this amorphous state at *T*g, as it can enhance the desired drug's properties, such as solubility and stability.

Although *T*g is conventionally associated with amorphous materials, certain crystalline APIs or their solid-state intermediates can exhibit transitions akin to *T*g under specific conditions, such as in the presence of residual solvents or during processing steps that induce partial disorder (Descamps & Willart, 2016; Newman & Zografi, 2020). However, these transitions in crystalline materials are limited and often less pronounced than those observed in purely amorphous forms (Shuang et al*.,* 2025; Wieczerzak et al*.*, 2023). Any apparent "*T*g-like" transitions typically stem from non-crystalline domains or interacting impurities (Wieczerzak et al., 2023). Because these transitions are weaker and less predictable, relying on them to improve solubility or stability is often insufficient. This is one reason why formulators turn to ASDs or other advanced formulation approaches to impart a controlled amorphous character,

enhance solubility, and achieve the necessary therapeutic outcomes (Pandi et al*.,* 2020; Patel et al*.,* 2022).

The formulation of ASDs involves careful selection of polymers and optimisation of the compound-polymer ratio to achieve the desired *T*g (Pandi et al., 2020; Schittny et al., 2020; Shi et al., 2022).

Recent work by Zhang et al. (2023) on indomethacin ASDs illustrated that increasing the polymer fraction in formulations with polyvinylpyrrolidone (PVP) not only raised the *T*g but also significantly retarded crystallisation. Their systematic investigation showed that a higher drug-polymer ratio led to enhanced intermolecular interactions, which translated into improved physical stability and a prolonged supersaturation state during dissolution. Similarly, Huang et al. (2024) optimized itraconazole ASDs using Soluplus®, demonstrating that careful adjustment of the compound-polymer ratio could be used to target a specific *T*g. Their findings confirmed that achieving an optimal *T*g was directly correlated with enhanced kinetic stability and a controlled drug release profile.

In a complementary study, Lee et al. (2021) investigated curcumin ASDs formulated with PVP K30. By systematically varying the drug loading, they were able to tailor the *T*g of the dispersions, which in turn impacted the dissolution behaviour and long-term stability of curcumin. The study highlighted that even small adjustments in polymer content can shift the *T*g sufficiently to suppress molecular mobility and inhibit recrystallisation. Together, these studies reinforce the critical role of polymer selection and the precise optimisation of drug-to-polymer ratios in designing robust ASDs with the desired thermal and physical properties.

2.4.1 Theoretical Estimation of *T*g in Polymer-Drug Mixtures

Several models for estimating the *T*g of polymer-drug mixtures exist such as the Fox, Couchman-Karasz and Kwei equations. However, the most popular model is the Gordon-Taylor equation (Equation 2.1). This equation is often applied to predict the *T*g of binary mixtures based on the weight fractions and individual *T*g of the components, providing a starting point for formulation design (Schugmann & Foerst, 2022; Weng et al*.*, 2013).

$$Tg = \frac{w1Tg1 + kw2Tg2}{w1 + kw2} \qquad \text{Equation (2.1)}$$

Where:

- *T*g is the glass transition temperature of the mixture
- *w1* and *w*2 are the weight fractions of the two components
- *T*g1 and *T*g2 are the glass transition temperatures of the individual components
- *k* reflects an interaction parameter between the two components and is also influenced by their respective densities and heat capacities or can be based on the ratio of polymer to compound used in binary ASDs

Studies have demonstrated that the solubility and bioavailability of poorly soluble APIs, such as nifedipine and carbamazepine, can be significantly improved through the formulation of ASDs using suitable polymers like PVPVA or Soluplus®. These investigations utilised *T*g predictions to systematically select optimal hot-melt extrusion conditions and to fine-tune the polymer-to-drug ratios. By employing *T*g-based methodologies, the research successfully identified formulation parameters that maximised drug stability and maintained the amorphous state, resulting in superior dissolution profiles compared to crystalline drug forms. This approach underscores the critical role that thermal analysis and predictive modelling play in the effective formulation of ASDs, particularly in enhancing solubility and therapeutic efficacy of challenging drug compounds (Djuris et al., 2013; Nair et al., 2020). Knowing a target *T*g assists in selecting process parameters that will preserve the amorphous state post-extrusion, thereby enhancing dissolution profiles and bioavailability (Gala et al., 2020; Moseson et al., 2024; Park et al., 2020). Another notable example involves naproxen-HPMC dispersions. Investigations have reported that *T*g values predicted by the Gordon-Taylor model closely match experimental data, providing a robust framework to fine-tune the polymer content and ensure the ASD's stability under varying temperature and humidity conditions (Iemtsev et al., 2020; LaFountaine et al., 2016). Adjusting the polymer proportion according to the predicted *T*g has proven effective in maintaining the drug's amorphous state and avoiding recrystallisation during storage (Bhujbal et al., 2021; Iyer et al., 2021; Pandi et al., 2020; Zhang et al., 2023).

2.5 Analysis of *T*g by DSC, mDSC and DSC-TGA

The *T*g can be measured by DSC since this instrumental technique can measure changes in the thermal environment of a formulation due to changes in the molecular mobility. Poorly homogeneous mixtures or physical mixtures have been known to show multiple *T*g's aligned closely with that of its individual components (Newman & Zografi, 2020). Some poorly water-soluble drugs have been shown to exhibit a single well-defined *T*g at a temperature applicable to the components in question in DSC depending on the stability of the amorphous structure rather than multiple *T*gs which may result from phase separation and poor miscibility, indicating a homogeneous amorphous matrix (Bhujbal et al., 2021; Simões et al., 2019; Tambe

et al., 2022). DSC assesses drug-polymer interactions by analysing thermal transitions, particularly shifts in the *T*g and melting endotherms. For instance, in the study by Meng et al. (2019), DSC was employed to evaluate interactions between celecoxib and polymers such as PVP. The authors observed a notable elevation of the *T*g temperature in polymer-rich amorphous solid dispersions, which indicated strong intermolecular interactions between celecoxib and PVP. These enhanced interactions were associated with improved physical stability and reduced recrystallisation of the drug, ultimately leading to significantly higher dissolution rates compared to formulations with weaker drug-polymer interactions. Thus, DSC serves as a sensitive tool for determining interaction strength and predicting formulation performance which influence both stability and dissolution kinetics. Additionally, in a review by Thayumanasundaram et al. (2022), PVPVA was highlighted as an effective polymer used in ASDs to substantially elevate the *T*g of formulations. For example, indomethacin, which originally exhibits a relatively low *T*g of approximately 42°C, displayed a significant *T*g increase upon formulation with PVPVA, achieving a higher *T*g of about 90°C. This pronounced elevation was attributed to robust molecular interactions, such as hydrogen bonding between the polymer and the drug molecules. Consequently, these interactions greatly restricted the molecular mobility of the amorphous drug, thereby significantly enhancing physical stability and reducing the formulation's susceptibility to recrystallisation during storage and handling. This effect underscores the importance of polymer choice and its role in stabilising amorphous drug formulations through targeted modifications of thermal characteristics.

Traditional DSC methods, however, combine all thermal processes, both kinetic (time-dependent) and thermodynamic (equilibrium), into a thermogram which can sometimes overlap with the *T*g of a formulation (Gill et al., 2010). Therefore, mDSC is used to remove these interferences so that the *T*g can be obtained. Studies exploring ASDs of hydrochlorothiazide or simvastatin with PVPVA and other polymeric excipients have illustrated that mDSC can detect subtle shifts in *T*g that would otherwise be masked by other thermal events such as secondary relaxations (Myślińska et al., 2023; Iyer et al., 2021; Macêdo et al., 2001).

Modulated differential scanning calorimetry (mDSC) has proven particularly useful beyond simply quantifying the *T*g; it provides valuable insights into subtle changes in *T*g related to storage conditions, humidity exposure, and physical aging of ASDs. mDSC can effectively separate complex thermal signals into reversible (*T*g-related) and non-reversible (physical aging, relaxation, and recrystallisation-related) heat flows. This capability allows researchers to detect minor shifts in *T*g and identify early signs of instability such as enthalpy relaxation and moisture-induced plasticisation, which traditional DSC might overlook due to overlapping thermal events. Consequently, employing mDSC facilitates a deeper understanding of how

environmental factors impact the long-term stability and performance of ASDs, thus guiding formulation optimisation and shelf-life predictions more accurately (Lappalainen & Karppinen, 2010).

Thermogravimetric analysis (TGA) evaluates a formulation's thermal stability and moisture content by monitoring weight loss as a function of temperature. Coupling a TGA to a DSC can further identify degradation temperatures, solvent residues, or moisture uptake that might compromise stability of the formulation (Chan, 2015; Dourado, 2019; Macêdo et al*.,* 2001; M. K. Singh & Singh, 2022). Nimodipine PVP based ASDs were found to have subtle but measurable mass losses when analysed using combined DSC and TGA analysis. These losses primarily stem from residual solvents and absorbed moisture within the dispersion. Such residual solvents or moisture may negatively impact the thermal properties of the ASD by reducing its *T*g and consequently increasing molecular mobility, thus elevating the risk of recrystallisation. DSC-TGA analysis, therefore, plays a role in identifying and quantifying these volatile components, facilitating optimal drying procedures, and improving the overall stability and shelf-life of the formulation (Rusdin et al., 2024; Zhang et al., 2023). The DSC scans revealed a distinct *T*g while information obtained from TGA determined temperatures that might provoke degradation or solvent evaporation (Rusdin et al*.,* 2024; Zhang et al., 2023). Similarly, for studies involving atorvastatin ASDs prepared with hydrophilic carriers such as HPMC and sodium lauryl sulfate (SLS), DSC and TGA have been employed to elucidate drug-polymer interactions and assess formulation stability. For instance, DSC thermograms of these ASDs typically reveal the absence of atorvastatin's characteristic crystalline melting peak, indicating a successful transition to the amorphous state. Concurrently, TGA data demonstrate minimal weight loss, suggesting low residual solvent content and enhanced thermal stability of the dispersion. These thermal analyses collectively confirm the formation of a homogeneous amorphous matrix, wherein molecular interactions between atorvastatin and the hydrophilic carriers contribute to improved physical stability and dissolution profiles (Kim et al*.,* 2013; Kwon et al*.,* 2019).

2.6 Analysis of ASDs by XRPD

The degree of crystallinity or the lack thereof in ASDs can be determined by XRPD. Previous literature provides illustrative examples of XRPD's value in ASD research. An ASD formulation of olanzapine with PVP confirmed the lack of olanzapine's crystallinity by the absence of sharp Bragg peaks indicating successful amorphisation (Chiang et al., 2023). Studies on lurasidone ASDs further leveraged XRPD to track changes in crystallinity after processing steps like spray drying or HME where researchers sought to examine presence or absence of crystalline properties such as Bragg peaks over time, ensuring that optimal processing conditions

prevented recrystallisation (Chiang et al., 2023; Jacob et al*.,* 2025). Again, in the formulation of felodipine ASDs with various carriers, XRPD analysis revealed the absence of sharp diffraction peaks, indicating the transformation of felodipine into its amorphous form within the dispersion (Mora-Castaño et al., 2024). This amorphisation was associated with enhanced dissolution rates compared to the crystalline drug. In a case with the study involving apremilast solid dispersions prepared using microwave-assisted techniques, the disappearance of characteristic crystalline peaks of apremilast was demonstrated through XRPD confirming its amorphous state in the formulations (Yang et al*.,* 2021).

2.7 Solubility and Dissolution of ASDs

A solubility experiment is performed by placing a formulation in a solvent at a fixed time and temperature. The amount of compound dissolved in the solvent is a key indicator of its solubility. A dissolution study follows a solubility study and is performed in a solvent too, sometimes at varying pH to simulate GI tract conditions. The solvent media is sampled at different time points to establish a dissolution rate (Pandi et al., 2020; Rusdin et al*.,* 2024).

ASDs can enhance the bioavailability of poorly water-soluble drugs by generating supersaturated solutions during dissolution, leading to increased drug concentrations in the gastrointestinal tract. Gan et al. (2023) reported that an amorphous dispersion of paclitaxel achieved ~100-fold supersaturation for over 2 hours, yielding ~1.78× higher oral bioavailability than the crystalline form. Although supersaturated solutions risk precipitation, studies show that drug-rich nanodroplets formed during liquid-liquid phase separation can serve as reservoirs to maintain drug levels and aid absorption, meaning sustained supersaturation can indeed improve bioavailability (Brouwers et al*.,* 2009; Gan et al*.,* 2023; Kong et al*.,* 2023).

Multiple studies have documented the clear impact of ASDs on improving solubility and dissolution rates. For example, the incorporation of poorly soluble compounds such as itraconazole into polymeric carriers like HPMC or HPMC-AS has been shown to produce ASDs that maintain the drug in a non-crystalline form, resulting in higher dissolution rates and prolonged supersaturation (Darwich et al*.,* 2023; Huang et al*.,* 2024; Mishra et al*.,* 2022; W. Zhang et al., 2024). Similarly, Boyd et al. (2019) and Czajkowski et al. (2023) discussed how the selection of appropriate polymers such as PVP/VA and polymer alternatives such as the use of phospholipid PHOSPHOLIPON 90H® with processing methods such as batch melting with DSC, can enhance the dissolution profile of drugs like fenofibrate and posaconazole which would otherwise be limited by low inherent solubility. In another example, Kyerematen et al. (2022) demonstrated that hot melt-extruded ASDs of posaconazole in HPMC-AS not only improved dissolution under biorelevant conditions, which more closely simulate dissolution testing environments found in GI fluids by mimicking this environment *in vitro*, but

also maintained supersaturation for extended period, offering enhanced permeability and absorption potential.

Environmental conditions such as temperature, pH, and the presence of moisture can significantly affect the solubility and stability of ASDs (Bhujbal et al., 2021; Iyer et al*.,* 2021; Pandi et al*.,* 2020; Zhang et al*.,* 2023). In many instances, the use of PVP or PVPVA stabilised the amorphous form, reduced recrystallisation tendencies and allowed for sustained drug integrity past the harsh conditions of the GI system thus offering consistent drug concentrations in solution (Bhujbal et al., 2021; Hiew et al*.,* 2022; Rusdin et al., 2024; Zhang et al., 2023). In these instances, dissolution rate is often compared against the crystalline form of the drug as a control (Bhujbal et al*.,* 2021; Hiew et al., 2022; Rusdin et al*.,* 2024; Zhang et al*.,* 2023). For instance, research on curcumin ASDs formulated with PVP demonstrated complete dissolution within 30 minutes in 0.1 N HCl, whereas the crystalline counterpart exhibited negligible release over a 90-minute period, highlighting the significant enhancement in dissolution rate conferred by the amorphous formulation (Zhang et al., 2023). The formulation factors including the choice of polymer, drug-polymer ratio, and the method of ASD preparation (e.g., solvent evaporation, melt extrusion) are crucial for optimising the dissolution profile and physical stability of the ASD (Tambe et al*.,* 2022).

The optimisation of ASDs necessitates meticulous selection of formulation parameters, including the choice of polymer, drug-to-polymer ratio, and preparation method, as these factors critically influence the dissolution profile and physical stability of the final product. For instance, in the development of ASDs for flubendazole, the incorporation of specific adjuvants and careful adjustment of drug loading were pivotal in achieving enhanced dissolution rates and maintaining amorphous stability (De Assis et al., 2022). Similarly, studies on apremilast ASDs have demonstrated that the type of polymer employed significantly affects the system's ability to sustain supersaturation and inhibit recrystallisation, thereby ensuring consistent bioavailability (Yang et al., 2021). Furthermore, the selection of the preparation technique, such as spray drying versus hot-melt extrusion, has been shown to impact the microstructure and residual solvent content of ASDs, which in turn affects their dissolution behaviour and storage stability (Simões et al., 2019). These examples underscore the necessity of a comprehensive understanding of formulation variables to tailor ASDs that meet desired therapeutic outcomes (De Assis et al., 2022; Pandi et al*.,* 2020; Shetty et al., 2023).

2.7.1 Polymer Ratios and Dissolution

The ratio of polymer to drug (Table 2.1) within an ASD largely influences the modulation of both solubility and dissolution behaviour, as it directly affects the stability of the amorphous phase and the extent of supersaturation achieved in aqueous media (Iyer et al., 2021; Pöstges

et al., 2023). Darwich et al. (2023) reported that higher polymer-to-drug ratios in ASDs of poorly soluble drugs, such as itraconazole, show potential to extend overall stability of the ASD through bonding interactions and molecular dispersion and further this improved their supersaturation capabilities leading to increased solubility. The choice of processing technique and incorporation of milling further led to the success of high polymer ratio ASDs (Darwich et al. 2023).

Table 2.1: Drug-to-Polymer Ratio Comparisons and their effects on Drug Availability

Polymer	**Drug**	**Drug-to-Polymer Ratio**	**Effect on Drug Availability**	**Reference**
Polyvinylpyrrolidone	Nimodipine	2:1	Enhanced dissolution rate and stability compared to PVPVA and Soluplus formulations.	Sun et al., 2019
Polyvinylpyrrolidone vinyl acetate	Indomethacin	1:1	Improved dissolution; however, less effective in suppressing crystallization compared to PVP.	Patel & Anderson, 2015
Soluplus®	Diosgenin	1:4	Significant improvement in aqueous solubility and bioavailability attributed to amorphisation and molecular interactions.	Liu et al., 2020
Hydroxypropyl Methylcellulose	Curcumin	1:4	Significant enhancement in solubility and dissolution rate compared to pure drug, attributed to the formation of amorphous solid dispersion.	Ishtiaq et al., 2022
Hydroxypropyl Methylcellulose Acetate Succinate	Celecoxib	1:4	Enhanced dissolution performance and precipitation inhibition, leading to improved bioavailability.	Monschke & Wagner, 2020

Eudragit® L100-55	Apalutamide	1:4	Enhanced dissolution profiles and physical stability, with the polymer acting as a precipitation inhibitor.	Sapkal et al., 2024
Kollidon® VA 64	Rivaroxaban	1:4	Improved dissolution behaviour and bioavailability, maintaining the drug in an amorphous state.	Kožák et al., 2022
Polyvinylpyrrolidone	Alpha-mangostin	1:4	Enhanced dissolution profile and physical stability due to hydrogen bonding interactions between drug and polymer.	Budiman et al., 2023
Polyvinylpyrrolidone vinyl acetate	Ritonavir	1:4	Improved dissolution rate and physical stability, maintaining amorphous form and preventing recrystallisation.	Krummnow et al., 2022
Eudragit® L100	Nintedanib	1:4	Increased drug solubility and maintained supersaturation, resulting in enhanced oral absorption.	Qin et al., 2022

2.8 Conclusion

In summary, the literature indicates that dispersion of poorly water-soluble APIs into polymer matrices can raise the free-energy state, generate supersaturation, and suppress crystallisation, thereby improving dissolution performance. Polymer choice (e.g., PVP K25) and process selection (e.g., solvent evaporation or HME) determine whether a single-phase amorphous system with a characteristic Tg is achieved and maintained during storage. The analytical toolkit (DSC/mDSC, XRPD, PLM, UV-Vis) provides orthogonal evidence for amorphisation, miscibility and stability. These principles guided the design of the present formulation and the selection of methods used to characterise the chloroquinoline derivative ASD.

Reference List

Andrews, G. P., Qian, K., Jacobs, E., Jones, D. S., & Tian, Y. (2023). High drug loading nanosized amorphous solid dispersion (NASD) with enhanced in vitro solubility and permeability: Benchmarking conventional ASD. International Journal of Pharmaceutics, 632, 122551. https://doi.org/10.1016/J.IJPHARM.2022.122551

Bhujbal, S. V., Mitra, B., Jain, U., Gong, Y., Agrawal, A., Karki, S., Taylor, L. S., Kumar, S., & Zhou, T., (2021). Pharmaceutical amorphous solid dispersion: A review of manufacturing strategies. Acta Pharmaceutica Sinica B, 11(8), 2505–2536. https://doi.org/10.1016/J.APSB.2021.05.014

Billinge, S. J. L. (2019). The rise of the X-ray atomic pair distribution function method: a series of fortunate events. Philosophical Transactions of the Royal Society A, 377(2147). https://doi.org/10.1098/RSTA.2018.0413

Bohg, C., Öster, C., Utesch, T., Bischoff, S., Lange, S., Shi, C., Sun, H., & Lange, A. (2021). A combination of solid-state NMR and MD simulations reveals the binding mode of a rhomboid protease inhibitor. Chemical Science, 12(38), 12754. https://doi.org/10.1039/D1SC02146J

Boyd, B. J., Bergström, C. A. S., Vinarov, Z., Kuentz, M., Brouwers, J., Augustijns, P., Brandl, M., Bernkop-Schnürch, A., Shrestha, N., Préat, V., Müllertz, A., Bauer-Brandl, A., & Jannin, V. (2019). Successful oral delivery of poorly water-soluble drugs both depends on the intraluminal behavior of drugs and of appropriate advanced drug delivery systems. European Journal of Pharmaceutical Sciences, 137, 104967. https://doi.org/10.1016/J.EJPS.2019.104967

Brouwers, J., Brewster, M. E., & Augustijns, P. (2009). Supersaturating drug delivery systems: The answer to solubility-limited oral bioavailability? Journal of Pharmaceutical Sciences, 98(8), 2549–2572. https://doi.org/10.1002/JPS.21650

Budiman, A., Nurani, N. V., Laelasari, E., Muchtaridi, M., Sriwidodo, S., & Aulifa, D. L. (2023). Effect of Drug-Polymer Interaction in Amorphous Solid Dispersion on the Physical Stability and Dissolution of Drugs: The Case of Alpha-Mangostin. Polymers, 15(14), 3034. https://doi.org/10.3390/POLYM15143034/S1

Chan, S. Y., Qi, S., & Craig, D. Q. M. (2015). An investigation into the influence of drug-polymer interactions on the miscibility, processability and structure of polyvinylpyrrolidone-based hot melt extrusion formulations. International Journal of Pharmaceutics, 496(1), 95–106. https://doi.org/10.1016/J.IJPHARM.2015.09.063

Chiang, C. W., Lubach, J. W., Chen, T., Chin, S., Ly, J., Zhang, W., Hou, H. H., & Nagapudi, K. (2023). Development of an Amorphous Solid Dispersion Formulation for Mitigating Mechanical Instability of Crystalline Form and Improving Bioavailability for Early Phase Clinical Studies. Molecular Pharmaceutics, 20(5), 2452–2464. https://doi.org/10.1021/ACS.MOLPHARMACEUT.2C01056

Czajkowski, M., Jacobsen, A. C., Bauer-Brandl, A., Brandl, M., & Skupin-Mrugalska, P. (2023). Hydrogenated phospholipid, a promising excipient in amorphous solid dispersions of fenofibrate for oral delivery: Preparation and in-vitro biopharmaceutical characterization. International Journal of Pharmaceutics, 644, 123294. https://doi.org/10.1016/J.IJPHARM.2023.123294

Dahan, A., Miller, J. M., & Amidon, G. L. (2009). Prediction of Solubility and Permeability Class Membership: Provisional BCS Classification of the World's Top Oral Drugs. The AAPS Journal, 11(4), 740. https://doi.org/10.1208/S12248-009-9144-X

Darwich, M., Mohylyuk, V., Kolter, K., Bodmeier, R., & Dashevskiy, A. (2023). Enhancement of itraconazole solubility and release by hot-melt extrusion with Soluplus®. Journal of Drug Delivery Science and Technology, 81, 104280. https://doi.org/10.1016/J.JDDST.2023.104280

De Assis, J. M. C., Barbosa, E. J., Bezzon, V. D. N., Lourenço, F. R., Carvalho, F. M. S., Matos, J. R., Araci Bou-Chacra, N., Benmore, C. J., Byrn, S. R., Costa, F. N., & de Araujo, G. L. B. (2022). Hot-melt extrudability of amorphous solid dispersions of flubendazole-copovidone: An exploratory study of the effect of drug loading and the balance of adjuvants on extrudability and dissolution. International Journal of Pharmaceutics, 614, 121456. https://doi.org/10.1016/J.IJPHARM.2022.121456

Debenedetti, P. G., & Stillinger, F. H. (2001). Supercooled liquids and the glass transition. www.nature.com

Descamps, M., & Willart, J. F. (2016). Perspectives on the amorphisation/milling relationship in pharmaceutical materials. Advanced Drug Delivery Reviews, 100, 51–66. https://doi.org/10.1016/J.ADDR.2016.01.011

Djuris, J., Nikolakakis, I., Ibric, S., Djuric, Z., & Kachrimanis, K. (2013). Preparation of carbamazepine-Soluplus® solid dispersions by hot-melt extrusion, and prediction of drug-polymer miscibility by thermodynamic model fitting. European Journal of Pharmaceutics and Biopharmaceutics : Official Journal of Arbeitsgemeinschaft Fur Pharmazeutische Verfahrenstechnik e.V, 84(1), 228–237. https://doi.org/10.1016/J.EJPB.2012.12.018

Dyre, J. C. (2006). Colloquium: The glass transition and elastic models of glass-forming liquids. https://doi.org/10.1103/RevModPhys.78.953

Dourado, D. (2019). Thermal Analysis as a Useful Tool in Drug-Excipient Compatibilty Studies: The Impact in Pharmaceuticals Products. Biomedical Journal of Scientific & Technical Research, 22(3). https://doi.org/10.26717/BJSTR.2019.22.003745

Einfalt, T.; Planinšek, O.; Hrovat, K. (2013). Methods of amorphization and investigation of the amorphous state. Acta Pharmaceutica, 63, 305–334. Figure 1 in this paper is a “Schematic representation of the structure of an amorphous and a crystalline solid” and matches your diagram concept.

Fayed, N. D., Arafa, M. F., Essa, E. A., & El Maghraby, G. M. (2022). Lopinavir-menthol co-crystals for enhanced dissolution rate and intestinal absorption. Journal of Drug Delivery Science and Technology, 74, 103587. https://doi.org/10.1016/J.JDDST.2022.103587

Figueiredo, J., Mendes, M., Pais, A., Sousa, J., & Vitorino, C. (2024). Microfluidics-on-a-chip for designing celecoxib-based amorphous solid dispersions: when the process shapes the product. Drug Delivery and Translational Research, 1–21. https://doi.org/10.1007/S13346-024-01633-7/TABLES/13

Gala, U., Miller, D., & Williams, R. O. (2020). Improved Dissolution and Pharmacokinetics of Abiraterone through KinetiSol® Enabled Amorphous Solid Dispersions. Pharmaceutics, 12(4), 357. https://doi.org/10.3390/PHARMACEUTICS12040357

Gan, Y., Baak, J. P. A., Chen, T., Ye, H., Liao, W., Lv, H., Wen, C., & Zheng, S. (2023). Supersaturation and Precipitation Applicated in Drug Delivery Systems: Development Strategies and Evaluation Approaches. Molecules, 28(5), 2212. https://doi.org/10.3390/MOLECULES28052212

Gill, P., Moghadam, T. T., & Ranjbar, B. (2010). Differential Scanning Calorimetry Techniques: Applications in Biology and Nanoscience. Journal of Biomolecular Techniques : JBT, 21(4), 167. https://pmc.ncbi.nlm.nih.gov/articles/PMC2977967/

Gulsun, T., Borna, S. E., Vural, I., & Sahin, S. (2018). Preparation and characterization of furosemide nanosuspensions. Journal of Drug Delivery Science and Technology, 45, 93–100. https://doi.org/10.1016/J.JDDST.2018.03.005

Hamed, R., Mohamed, E. M., Sediri, K., Khan, M. A., & Rahman, Z. (2021). Development of stable amorphous solid dispersion and quantification of crystalline fraction of lopinavir by spectroscopic-chemometric methods. International Journal of Pharmaceutics, 602, 120657. https://doi.org/10.1016/J.IJPHARM.2021.120657

Healy, A. M., Worku, Z. A., Kumar, D., & Madi, A. M. (2017). Pharmaceutical solvates, hydrates and amorphous forms: A special emphasis on cocrystals. Advanced Drug Delivery Reviews, 117, 25–46. https://doi.org/10.1016/J.ADDR.2017.03.002

Hiew, T. N., Zemlyanov, D. Y., & Taylor, L. S. (2022). Balancing Solid-State Stability and Dissolution Performance of Lumefantrine Amorphous Solid Dispersions: The Role of Polymer Choice and Drug-Polymer Interactions. Molecular Pharmaceutics, 19(2), 392–413. https://doi.org/10.1021/ACS.MOLPHARMACEUT.1C00481/ASSET/IMAGES/LARGE/MP1C00481_0013.JPEG

Holm, T. P., Knopp, M. M., Berthelsen, R., & Löbmann, K. (2022). Supersaturated amorphous solid dispersions of celecoxib prepared in situ by microwave irradiation. International Journal of Pharmaceutics, 626, 122115. https://doi.org/10.1016/J.IJPHARM.2022.122115

Huang, L., Guo, J., Li, Y., Yang, W., Ni, W., Jia, Y., Yu, M., & Zhang, J. (2024). Improve Solubility and Develop Personalized Itraconazole Dosages via Forming Amorphous Solid Dispersions with Hydrophilic Polymers Utilizing HME and 3D Printing Technologies. Polymers, 16(23), 3302. https://doi.org/10.3390/POLYM16233302/S1

Iemtsev, A., Hassouna, F., Mathers, A., Klajmon, M., Dendisová, M., Malinová, L., Školáková, T., & Fulem, M. (2020). Physical stability of hydroxypropyl methylcellulose-based amorphous solid dispersions: Experimental and computational study. International Journal of Pharmaceutics, 589. https://doi.org/10.1016/J.IJPHARM.2020.119845

Ishtiaq, M., Asghar, S., Khan, I. U., Iqbal, M. S., & Khalid, S. H. (2022). Development of the Amorphous Solid Dispersion of Curcumin: A Rational Selection of Polymers for Enhanced Solubility and Dissolution. Crystals 2022, Vol. 12, Page 1606, 12(11), 1606. https://doi.org/10.3390/CRYST12111606

Iyer, R., Jovanovska, V. P., Berginc, K., Jaklič, M., Fabiani, F., Harlacher, C., Huzjak, T., & Sanchez-Felix, M. V. (2021). Amorphous Solid Dispersions (ASDs): The Influence of Material Properties, Manufacturing Processes and Analytical Technologies in Drug Product Development. Pharmaceutics, 13(10), 1682. https://doi.org/10.3390/PHARMACEUTICS13101682

Jacob, S., Kather, F. S., Boddu, S. H. S., Attimarad, M., & Nair, A. B. (2025). Nanosuspension Innovations: Expanding Horizons in Drug Delivery Techniques. Pharmaceutics, 17(1), 136. https://doi.org/10.3390/PHARMACEUTICS17010136

Jones, D. S., Margetson, D. N., McAllister, M. S., Yu, T., Shu, L., McCoy, C. P., & Andrews, G. P. (2014). Thermodynamically stable amorphous drug dispersions in amorphous hydrophilic

polymers engineered by hot melt extrusion. Chemical Engineering Research and Design, 92(12), 3046–3054. https://doi.org/10.1016/J.CHERD.2014.08.022

Jones, E. C. L., & Bimbo, L. M. (2020). Crystallisation Behaviour of Pharmaceutical Compounds Confined within Mesoporous Silicon. Pharmaceutics, 12(3), 214. https://doi.org/10.3390/PHARMACEUTICS12030214

Kong, Y., Wang, W., Wang, C., Li, L., Peng, D., & Tian, B. (2023). Supersaturation and phase behavior during dissolution of amorphous solid dispersions. International Journal of Pharmaceutics, 631. https://doi.org/10.1016/J.IJPHARM.2022.122524

Kožák, J., Chrétien, C., Pellequer, Y., & Lamprecht, A. (2022). Rivaroxaban lyospheres prepared by a dimethyl sulfoxide-based spray-freeze-drying process. International Journal of Pharmaceutics, 627, 122235. https://doi.org/10.1016/J.IJPHARM.2022.122235

Kim, M. S., Kim, J. S., Cho, W., Park, H. J., & Hwang, S. J. (2013). Oral absorption of atorvastatin solid dispersion based on cellulose or pyrrolidone derivative polymers. International Journal of Biological Macromolecules, 59, 138–142. https://doi.org/10.1016/J.IJBIOMAC.2013.03.068

Krstić, M., Manić, L., Martić, N., Vasiljević, D., Mračević, S. Đ., Vukmirović, S., & Rašković, A. (2020). Binary polymeric amorphous carvedilol solid dispersions: In vitro and in vivo characterization. European Journal of Pharmaceutical Sciences, 150, 105343. https://doi.org/10.1016/J.EJPS.2020.105343

Krummnow, A., Danzer, A., Voges, K., Dohrn, S., Kyeremateng, S. O., Degenhardt, M., & Sadowski, G. (2022). Explaining the Release Mechanism of Ritonavir/PVPVA Amorphous Solid Dispersions. Pharmaceutics, 14(9), 1904. https://doi.org/10.3390/PHARMACEUTICS14091904/S1

Kwon, J., Giri, B. R., Song, E. S., Bae, J., Lee, J., & Kim, D. W. (2019). Spray-Dried Amorphous Solid Dispersions of Atorvastatin Calcium for Improved Supersaturation and Oral Bioavailability. Pharmaceutics, 11(9), 461. https://doi.org/10.3390/PHARMACEUTICS11090461

Kyeremateng, S. O., Voges, K., Dohrn, S., Sobich, E., Lander, U., Weber, S., Gessner, D., Evans, R. C., & Degenhardt, M. (2022). A Hot-Melt Extrusion Risk Assessment Classification System for Amorphous Solid Dispersion Formulation Development. Pharmaceutics, 14(5), 1044. https://doi.org/10.3390/PHARMACEUTICS14051044/S1

LaFountaine, J. S., Prasad, L. K., Brough, C., Miller, D. A., McGinity, J. W., & Williams, R. O. (2016). Thermal Processing of PVP- and HPMC-Based Amorphous Solid Dispersions. AAPS PharmSciTech, 17(1), 120–132. https://doi.org/10.1208/S12249-015-0417-7

Lappalainen, M., & Karppinen, M. (2010). Techniques of differential scanning calorimetry for quantification of low contents of amorphous phases. Journal of Thermal Analysis and Calorimetry, 102(1), 171–180. https://doi.org/10.1007/S10973-010-0817-6

Lee, J.-H., Sik Jeong, H., Jeong, J.-W., Koo, T.-S., Kim, D.-K., Cho, Y. H., Lee, G. W., Lee, C. :, Jeong, J.-H. ;, Jeong, H. S. ;, Koo, J.-W. ;, Kim, T.-S. ;, Cho, D.-K. ;, Lee, Y. H. ;, The, G. W., Kachrimanis, K., & Bilgili, E. (2021). The Development and Optimization of Hot-Melt Extruded Amorphous Solid Dispersions Containing Rivaroxaban in Combination with Polymers. Pharmaceutics, 13(3), 344. https://doi.org/10.3390/PHARMACEUTICS13030344

Liu, J., Grohganz, H., Löbmann, K., Rades, T., & Hempel, N. J. (2021). Co-Amorphous Drug Formulations in Numbers: Recent Advances in Co-Amorphous Drug Formulations with Focus on Co-Formability, Molar Ratio, Preparation Methods, Physical Stability, In Vitro and In Vivo Performance, and New Formulation Strategies. Pharmaceutics, 13(3). https://doi.org/10.3390/PHARMACEUTICS13030389

Liu, J., Li, Y., Ao, W., Xiao, Y., Bai, M., & Li, S. (2022). Preparation and Characterization of Aprepitant Solid Dispersion with HPMCAS-LF. ACS Omega, 7(44), 39907–39912. https://doi.org/10.1021/ACSOMEGA.2C04021/ASSET/IMAGES/LARGE/AO2C04021_0009.JPEG

Liu, P., Zhou, J. Y., Chang, J. H., Liu, X. G., Xue, H. F., Wang, R. X., Li, Z. S., Li, C. S., Wang, J., & Liu, C. Z. (2020). Soluplus-Mediated Diosgenin Amorphous Solid Dispersion with High Solubility and High Stability: Development, Characterization and Oral Bioavailability. Drug Design, Development and Therapy, 14, 2959. https://doi.org/10.2147/DDDT.S253405

Macêdo, R. O., Do Nascimento, T. G., & Veras, J. W. E. (2001). Comparison of generic hydrochlorothiazide formulations by means of TG and DSC coupled to a photovisual system. Journal of Thermal Analysis and Calorimetry, 64(2), 757–763. https://doi.org/10.1023/A:1011504730402

Maestrelli, F., Cirri, M., García-Villén, F., Borrego-Sánchez, A., Iborra, C. V., & Mura, P. (2020). Tablets of “Hydrochlorothiazide in Cyclodextrin in Nanoclay”: A New Nanohybrid System with Enhanced Dissolution Properties. Pharmaceutics, 12(2), 104. https://doi.org/10.3390/PHARMACEUTICS12020104

Martin-Pastor, M., & Stoyanov, E. (2021). New insights into the use of hydroxypropyl cellulose for drug solubility enhancement: An analytical study of sub-molecular interactions with fenofibrate in solid state and aqueous solutions. Journal of Polymer Science, 59(16), 1855–1865. https://doi.org/10.1002/POL.20210240

Melnyk, A., Junk, M. J. N., McGehee, M. D., Chmelka, B. F., Hansen, M. R., & Andrienko, D. (2017). Macroscopic Structural Compositions of π-Conjugated Polymers: Combined Insights from Solid-State NMR and Molecular Dynamics Simulations. Journal of Physical Chemistry Letters, 8(17), 4155–4160. https://doi.org/10.1021/ACS.JPCLETT.7B01443/SUPPL_FILE/JZ7B01443_SI_001.PDF

Mendes, C., Buttchevitz, A., Kruger, J. H., Kratz, J. M., Simões, C. M. O., De Oliveira Benedet, P., Oliveira, P. R., & Silva, M. A. S. (2016). Inclusion complexes of hydrochlorothiazide and β-cyclodextrin: Physicochemical characteristics, in vitro and in vivo studies. European Journal of Pharmaceutical Sciences, 83, 71–78. https://doi.org/10.1016/J.EJPS.2015.12.015

Meng, F., Ferreira, R., & Zhang, F. (2019). Effect of surfactant level on properties of celecoxib amorphous solid dispersions. Journal of Drug Delivery Science and Technology, 49, 301–307. https://doi.org/10.1016/J.JDDST.2018.11.026

Mishra, S. M., Richter, M., Mejia, L., & Sauer, A. (2022). Downstream Processing of Itraconazole:HPMCAS Amorphous Solid Dispersion: From Hot-Melt Extrudate to Tablet Using a Quality by Design Approach. Pharmaceutics, 14(7), 1429. https://doi.org/10.3390/PHARMACEUTICS14071429/S1

Monschke, M., & Wagner, K. G. (2020). Impact of HPMCAS on the Dissolution Performance of Polyvinyl Alcohol Celecoxib Amorphous Solid Dispersions. Pharmaceutics, 12(6), 541. https://doi.org/10.3390/PHARMACEUTICS12060541

Moseson, D. E., Parker, A. S., Beaudoin, S. P., & Taylor, L. S. (2020). Amorphous solid dispersions containing residual crystallinity: Influence of seed properties and polymer adsorption on dissolution performance. European Journal of Pharmaceutical Sciences, 146, 105276. https://doi.org/10.1016/J.EJPS.2020.105276

Mora-Castaño, G., Millán-Jiménez, M., Niederquell, A., Schönenberger, M., Shojaie, F., Kuentz, M., & Caraballo, I. (2024). Amorphous solid dispersion of a binary formulation with felodipine and HPMC for 3D printed floating tablets. International Journal of Pharmaceutics, 658. https://doi.org/10.1016/J.IJPHARM.2024.124215

Myślińska, M., Stocker, M. W., Ferguson, S., & Healy, A. M. (2023). A Comparison of Spray-Drying and Co-Precipitation for the Generation of Amorphous Solid Dispersions (ASDs) of

Hydrochlorothiazide and Simvastatin. Journal of Pharmaceutical Sciences, 112(8), 2097–2114. https://doi.org/10.1016/J.XPHS.2023.02.012

Nair, A. R., Lakshman, Y. D., Anand, V. S. K., Sree, K. S. N., Bhat, K., & Dengale, S. J. (2020). Overview of Extensively Employed Polymeric Carriers in Solid Dispersion Technology. AAPS PharmSciTech, 21(8), 309. https://doi.org/10.1208/S12249-020-01849-Z

Newman, A., & Zografi, G. (2020). Commentary: Considerations in the Measurement of Glass Transition Temperatures of Pharmaceutical Amorphous Solids. AAPS PharmSciTech, 21(1). https://doi.org/10.1208/S12249-019-1562-1

Nguyen, D. N., & Van Den Mooter, G. (2014). The fate of ritonavir in the presence of darunavir. International Journal of Pharmaceutics, 475(1–2), 214–226. https://doi.org/10.1016/J.IJPHARM.2014.08.062

Nistane, J., Chen, L., Lee, Y., Lively, R., & Ramprasad, R. (2022). Estimation of the Flory-Huggins interaction parameter of polymer-solvent mixtures using machine learning. MRS Communications, 12(6), 1096–1102. https://doi.org/10.1557/S43579-022-00237-X

Pandi, P., Bulusu, R., Kommineni, N., Khan, W., & Singh, M. (2020). Amorphous solid dispersions: An update for preparation, characterization, mechanism on bioavailability, stability, regulatory considerations and marketed products. International Journal of Pharmaceutics, 586, 119560. https://doi.org/10.1016/J.IJPHARM.2020.119560

Papich, M. G., & Martinez, M. N. (2015). Applying Biopharmaceutical Classification System (BCS) Criteria to Predict Oral Absorption of Drugs in Dogs: Challenges and Pitfalls. The AAPS Journal, 17(4), 948. https://doi.org/10.1208/S12248-015-9743-7

Park, H., Ha, E. S., & Kim, M. S. (2020). Current Status of Supersaturable Self-Emulsifying Drug Delivery Systems. Pharmaceutics, 12(4), 365. https://doi.org/10.3390/PHARMACEUTICS12040365

Patel, D. D., & Anderson, B. D. (2015). Adsorption of Polyvinylpyrrolidone and its Impact on Maintenance of Aqueous Supersaturation of Indomethacin via Crystal Growth Inhibition. Journal of Pharmaceutical Sciences, 104(9), 2923–2933. https://doi.org/10.1002/JPS.24493

Patel, V., Patel, A., & Shah, A. (2023). Enhancing the dissolution rate of poorly soluble drug Febuxostat using spray dried amorphous solid dispersion technique. Ars Pharmaceutica (Internet), 64(2), 123–138. https://doi.org/10.30827/ARS.V64I2.27058

Patel, K., Shah, S., & Patel, J. (2022). Solid dispersion technology as a formulation strategy for the fabrication of modified release dosage forms: A comprehensive review. DARU Journal of Pharmaceutical Sciences, 30(1), 165. https://doi.org/10.1007/S40199-022-00440-0

Patil, H., Tiwari, R.V. & Repka, M.A. (2016). Hot-Melt Extrusion: from Theory to Application in Pharmaceutical Formulation. *AAPS PharmSciTech*, 17(1), 20–42. https://doi.org/10.1208/s12249-015-0360-7

Pires, M. A. S., Dos Santos, R. A. S., & Sinisterra, R. D. (2011). Pharmaceutical Composition of Hydrochlorothiazide:β-Cyclo-dextrin: Preparation by Three Different Methods, Physico-Chemical Characterization and In Vivo Diuretic Activity Evaluation. Molecules, 16(6), 4482. https://doi.org/10.3390/MOLECULES16064482

Pöstges, F., Kayser, K., Stoyanov, E., & Wagner, K. G. (2022). Boost of solubility and supersaturation of celecoxib via synergistic interactions of methacrylic acid-ethyl acrylate copolymer (1:1) and hydroxypropyl cellulose in ternary amorphous solid dispersions. International Journal of Pharmaceutics: X, 4, 100115. https://doi.org/10.1016/J.IJPX.2022.100115

Qin, Y., Xiao, C., Li, X., Huang, J., Si, L., & Sun, M. (2022). Enteric Polymer–Based Amorphous Solid Dispersions Enhance Oral Absorption of the Weakly Basic Drug Nintedanib via Stabilization of Supersaturation. Pharmaceutics, 14(9), 1830. https://doi.org/10.3390/PHARMACEUTICS14091830

Reppas, C., Kuentz, M., Bauer-Brandl, A., Carlert, S., Dallmann, A., Dietrich, S., Dressman, J., Ejskjaer, L., Frechen, S., Guidetti, M., Holm, R., Holzem, F. L., Karlsson, E., Kostewicz, E., Panbachi, S., Paulus, F., Senniksen, M. B., Stillhart, C., Turner, D. B., … O'Dwyer, P. J. (2023). Leveraging the use of in vitro and computational methods to support the development of enabling oral drug products: An InPharma commentary. European Journal of Pharmaceutical Sciences, 188, 106505. https://doi.org/10.1016/J.EJPS.2023.106505

Rusdin, A., Mohd Gazzali, A., Ain Thomas, N., Megantara, S., Aulifa, D. L., Budiman, A., & Muchtaridi, M. (2024). Advancing Drug Delivery Paradigms: Polyvinyl Pyrolidone (PVP)-Based Amorphous Solid Dispersion for Enhanced Physicochemical Properties and Therapeutic Efficacy. Polymers, 16(2). https://doi.org/10.3390/POLYM16020286

Samineni, R., Chimakurthy, J., & Konidala, S. (2022). Emerging Role of Biopharmaceutical Classification and Biopharmaceutical Drug Disposition System in Dosage form Development: A Systematic Review. Turkish Journal of Pharmaceutical Sciences, 19(6), 706. https://doi.org/10.4274/TJPS.GALENOS.2021.73554

Sapkal, R., Devangan, P., Madan, J., & Dikundwar, A. G. (2024). Neat Amorphous Form and Amorphous Solid Dispersions of Apalutamide: A Comparative Study. https://doi.org/10.2139/SSRN.5013722

Schittny, A., Huwyler, J., & Puchkov, M. (2019). Mechanisms of increased bioavailability through amorphous solid dispersions: a review. Drug Delivery, 27(1), 110. https://doi.org/10.1080/10717544.2019.1704940

Schugmann, M., & Foerst, P. (2022). Systematic Investigation on the Glass Transition Temperature of Binary and Ternary Sugar Mixtures and the Applicability of Gordon-Taylor and Couchman–Karasz Equation. Foods 2022, Vol. 11, Page 1679, 11(12), 1679. https://doi.org/10.3390/FOODS11121679

Shamsuddin, S., Fazil, M., Ansari, S., & Ali, J. (2016). Atorvastatin solid dispersion for bioavailability enhancement. Journal of Advanced Pharmaceutical Technology & Research, 7(1), 22. https://doi.org/10.4103/2231-4040.169873

Shetty, D., Yarlagadda, D. L., Brahmam, B., Dengale, S. J., & Lewis, S. A. (2023). Investigating the influence of the type of polymer on sustaining the supersaturation from amorphous solid dispersions of Apremilast and its pharmacokinetics. Journal of Drug Delivery Science and Technology, 84, 104520. https://doi.org/10.1016/J.JDDST.2023.104520

Shi, Q., Chen, H., Wang, Y., Wang, R., Xu, J., & Zhang, C. (2022). Amorphous Solid Dispersions: Role of the Polymer and Its Importance in Physical Stability and In Vitro Performance. Pharmaceutics, 14(8), 1747. https://doi.org/10.3390/PHARMACEUTICS14081747

Shi, Q., Li, F., Yeh, S., Wang, Y., & Xin, J. (2020). Physical stability of amorphous pharmaceutical solids: Nucleation, crystal growth, phase separation and effects of the polymers. International Journal of Pharmaceutics, 590, 119925. https://doi.org/10.1016/J.IJPHARM.2020.119925

Shuang, Y., Saito, Y., Hatayama, S., Fons, P., Daisuke, A., & Sutou, Y. (2025). Amorphous-to-crystalline transition-induced two-step thin film growth of quasi-one-dimensional penta-telluride ZrTe5. Journal of Materials Science & Technology, 210, 246–253. https://doi.org/10.1016/J.JMST.2024.05.039

Simões, M. F., Pinto, R. M. A., & Simões, S. (2019). Hot-melt extrusion in the pharmaceutical industry: toward filing a new drug application. Drug Discovery Today, 24(9), 1749–1768. https://doi.org/10.1016/J.DRUDIS.2019.05.013

Singh, M. K., & Singh, A. (2022). Thermogravimetric analyzer. Characterization of Polymers and Fibres, 223–240. https://doi.org/10.1016/B978-0-12-823986-5.00015-4

Sun, D. D., Ju, T. C. R., & Lee, P. I. (2012). Enhanced kinetic solubility profiles of indomethacin amorphous solid dispersions in poly(2-hydroxyethyl methacrylate) hydrogels. European Journal of Pharmaceutics and Biopharmaceutics, 81(1), 149–158. https://doi.org/10.1016/J.EJPB.2011.12.016

Sun, Z., Zhang, H., He, H., Sun, L., Zhang, X., Wang, Q., Li, K., & He, Z. (2019). Cooperative effect of polyvinylpyrrolidone and HPMC E5 on dissolution and bioavailability of nimodipine solid dispersions and tablets. Asian Journal of Pharmaceutical Sciences, 14(6), 668–676. https://doi.org/10.1016/J.AJPS.2018.08.005

Tambe, S., Jain, D., Meruva, S. K., Rongala, G., Juluri, A., Nihalani, G., Mamidi, H. K., Nukala, P. K., & Bolla, P. K. (2022). Recent Advances in Amorphous Solid Dispersions: Preformulation, Formulation Strategies, Technological Advancements and Characterization. Pharmaceutics, 14(10), 2203. https://doi.org/10.3390/PHARMACEUTICS14102203

Thayumanasundaram, S., Venkatesan, T. R., Ousset, A., Van Hollebeke, K., Aerts, L., Wübbenhorst, M., & Van Den Mooter, G. (2022). Complementarity of mDSC, DMA, and DRS Techniques in the Study of Tgand Sub- TgTransitions in Amorphous Solids: PVPVA, Indomethacin, and Amorphous Solid Dispersions Based on Indomethacin/PVPVA. Molecular Pharmaceutics, 19(7), 2299–2315. https://doi.org/10.1021/ACS.MOLPHARMACEUT.2C00123

Weng, L., Vijayaraghavan, R., MacFarlane, D. R., & Elliott, G. D. (2013). Application of the Kwei Equation tomodel the Tg Behavior of Binary Blends of Sugars and Salts. Cryobiology, 68(1), 155. https://doi.org/10.1016/J.CRYOBIOL.2013.12.005

Wieczerzak, K., Sharma, A., Hain, C., & Michler, J. (2023). Crystalline or amorphous? A critical evaluation of phenomenological phase selection rules. Materials & Design, 230, 111994. https://doi.org/10.1016/J.MATDES.2023.111994

Yang, L., Wu, P., Xu, J., Xie, D., Wang, Z., Wang, Q., Chen, Y., Li, C. H., Zhang, J., Chen, H., & Quan, G. (2021). Development of Apremilast Solid Dispersion Using TPGS and PVPVA with Enhanced Solubility and Bioavailability. AAPS PharmSciTech, 22(4). https://doi.org/10.1208/S12249-021-02005-X

Yun, T., Lee, S., Yun, S., Cho, D., Bang, K., & Kim, K. (2024). Investigation of Stabilized Amorphous Solid Dispersions to Improve Oral Olaparib Absorption. Pharmaceutics, 16(7), 958. https://doi.org/10.3390/PHARMACEUTICS16070958/S1

Zhang, J., Guo, M., Luo, M., & Cai, T. (2023). Advances in the development of amorphous solid dispersions: The role of polymeric carriers. Asian Journal of Pharmaceutical Sciences, 18(4), 100834. https://doi.org/10.1016/J.AJPS.2023.100834

Zhang, W., Huang, L., Guo, J., Li, Y., Yang, W., Ni, W., Jia, Y., Yu, M., & Zhang, J. (2024). Improve Solubility and Develop Personalized Itraconazole Dosages via Forming Amorphous Solid Dispersions with Hydrophilic Polymers Utilizing HME and 3D Printing Technologies. Polymers, 16(23), 3302. https://doi.org/10.3390/POLYM16233302

Zhu, J., Lin, L.-H., Niu, H., Shang, Q., Wang, Q., Yan, F., & Li, J.-J. (2025). Data-Driven Prediction of Flory–Huggins Parameter for Quantifying Polymer–Solvent Interaction. Industrial & Engineering Chemistry Research. https://doi.org/10.1021/ACS.IECR.4C04761

CHAPTER 3

The Characterisation and Solubility Improvement of a Novel Chloroquinoline Derivative in an Amorphous Solid Dispersion Formulation

N. Raghunandan[1], T. Moodley[1], W. Liebenberg[2]

[1]DSI/NWU Preclinical Drug Development Platform, Faculty of Health Sciences, North-West University, Potchefstroom, South Africa, 2521

[2]Centre of Excellence for Pharmaceutical Sciences, Faculty of Health Sciences, North-West University, Potchefstroom, South Africa, 2521

Abstract

This study aimed to improve the solubility of a novel chloroquinoline derivative by developing an amorphous solid dispersion (ASD) using polyvinylpyrrolidone (PVP K25) as a polymeric carrier. The ASD was prepared via a solvent evaporation method, followed by characterisation using Differential Scanning Calorimetry (DSC), Modulated DSC (MDSC), X-ray Powder Diffraction (XRPD), and Polarised Light Microscopy (PLM). A glass transition (*T*g) of 136.98°C degrees was obtained and a corresponding loss in ASD mass was observed between 40-80°C. MDSC demonstrated a potential structural relaxation or secondary relaxation thermal event. Solubility and dissolution studies, which were conducted using an aqueous and solid-state solubility method and USP apparatus 2 dissolution method respectively, showed a significant increase in these parameters within the ASD compared to the raw compound. These findings suggested that the ASD formulation is a promising approach to enhance the solubility and potentially improve the bioavailability of the chloroquinoline derivative.

3.1. Introduction

ASDs improve drug solubility by converting the drug to a higher-energy amorphous form within a polymer matrix, thus disrupting the crystalline lattice. In previous studies involving a host of popular drugs such as furosemide, nifedipine and ritonavir to name a few, a notable enhancement in bioavailability characteristics was found when the use of ASDs was employed (Bhujbal et al., 2021; Iyer et al., 2021; Zhang et al., 2023).

This study focuses on a novel chloroquinoline derivative which demonstrates potential activity against drug-resistant pathogens but suffers from low solubility (Perković et al., 2023). Several polymers exist that can potentially be used within an ASD system, each with their own properties that lend to the production of an ASD and the overall improvement of solubility. Some of the most commonly used include, PVP, HPMC, HPMC-AS, PVP/VA, Eudragit® series and PEG. PVP K25 was selected as the carrier polymer due to its

favourable *T*g temperature and known efficacy in stabilising amorphous forms as well as its widespread use in formulations and high miscibility (Asgreen et al., 2020; Rusdin et al., 2024). However, amorphous forms also present challenges due to their metastable nature, which can lead to recrystallisation under certain conditions such as elevated temperature or moisture exposure (Pandi et al., 2020; Strydom et al., 2009; Zhang et al., 2023). Despite these stability concerns, ASDs continue to be explored as a practical solution to overcome solubility limitations, especially for compounds that exhibit significant therapeutic potential but suffer from inadequate bioavailability.

Many approaches have been developed and used for producing ASDs, ranging from early physical mixing strategies to more advanced HME and spray drying techniques (Holm et al., 2022; Nguyen & Van Den Mooter., 2014). While these methods have successfully improved the solubility and stability of poorly soluble drugs (e.g., fenofibrate, celecoxib, and ritonavir), they can involve high processing temperatures or specialised equipment, which may limit their utility for thermally labile compounds (Fayed et al., 2022; Hamed et al., 2021). In contrast, solvent evaporation, via rotary evaporation, vacuum drying, or similar processes, provides a milder thermal profile and straightforward scale-up, allowing for consistent production of homogeneously amorphous dispersions with a clearly defined *T*g (Kim et al*.,* 2013; Kwon et al*.,* 2019; Shamsuddin et al*.,* 2016). Drugs such as atorvastatin have been formulated into stable ASDs through solvent evaporation, demonstrating substantially enhanced dissolution and bioavailability compared to their crystalline counterparts (Kim et al*.,* 2013). In this work, we therefore adopted a solvent evaporation approach to prepare an ASD of a novel chloroquinoline derivative with PVP K25, aiming to capitalise on its lower thermal stress and proven ability to yield robust, single-phase amorphous systems.

The objective of this study is to prepare an ASD of the chloroquinoline derivative using the solvent evaporation technique and characterise the resulting dispersion using various thermal, spectroscopic, and imaging techniques. The preliminary solubility and dissolution results highlight the solubility enhancement achieved through ASD formation.

3.2 Materials and Methods

3.2.1 Materials

The chloroquinoline derivative was synthesised at the University of Kwa-Zulu Natal's School of Chemistry and Physics (Durban, South Africa). Dimethyl sulfoxide,

dichloromethane (DCM), methanol, and hydrochloric acid were obtained from Merck Ltd. (Darmstadt, Germany). All reagents used were of analytical or chromatographic grade.

3.2.2 Preparation of the Amorphous Solid Dispersion

A physical mixture was made by combining 25 mg of the chloroquinoline derivative with 100 mg of PVP K25 via trituration. The mixture was then dissolved in 200 mL of DCM and stirred for 24 hours at ambient temperature to ensure homogeneity. DCM was evaporated using a rotary evaporator under reduced pressure, resulting in a thin film of the drug-polymer mixture. The thin film was dried in a vacuum oven at 60°C for 24 hours to remove any residual solvent. The resultant ASD was stored in a desiccator until further use.

3.3 Instrumentation

3.3.1 Miscibility Testing

A Mettler DSC 3^+ (Mettler Toledo, Greifensee, Switzerland) was used to record the DSC thermograms. Powder samples, weighing approximately 3 – 5 mg were placed in closed aluminium 40 µl cells and heated to an end temperature dependent on the melting point of the API and/or polymer, at a heating rate of 10^{o}C /min, with a nitrogen gas flow rate of 35 ml/min. The samples were then cooled down and subjected to the same thermal program once more.

3.3.2 Simultaneous Thermal Analysis (STA), Differential Scanning Calorimetry (DSC) and Modulated Differential Scanning Calorimetry (MDSC)

The thermal analysis was conducted using Mettler Toledo STARe software.

A Mettler DTG 3^+ (Mettler Toledo, Greifensee, Switzerland) was used to record the simultaneous thermal analysis i.e., the DSC and TGA thermograms. Powder samples, weighing approximately 5-8 mg were placed in open aluminum cells, (100 µl) and heated to an end temperature depending on the melting point of the API and/or polymer, at a heating rate of 10°C/min, with a nitrogen gas flow of 35 ml/min.

In the MDSC the sample was heated at 5°C /min from ambient to 190°C with a modulation amplitude of ±0.5°C every 30 seconds for a period of 60 seconds.

3.3.3 X-ray Powder Diffraction (XRPD)

Diffractograms were recorded using a Malvern Panalytical Empyrean X-ray diffractometer (Almelo, Netherlands) with a PIXcel^{3D} detector. XRPD patterns at ambient temperature with copper Kα source over a 2θ range of 5–40° (Table 3.1).

Table 3.1: XRPD Data Collection Parameters

Parameter	Value	Parameter	Value
Scan Axis	Gonio	K-Alpha1 (Å)	1.54060
Start Angle (2θ)	4.0033	K-Alpha2 (Å)	1.54443
End Angle (2θ)	39.9973	K-Beta (Å)	1.39225
Step Size (2θ)	0.0070	K-A2 / K-A1 Ratio	0.50000
Scan Step Time (s)	49.0820	Goniometer Radius (mm)	240.00
Anode material	Cu	Dist. Focus-Diverg. Slit (mm)	100.00
PSD Mode	Scanning	Incident Beam Monochromator	No
Generator settings	45 kV, 40 mA	Scan Type	Continuous
Diffractometer Type	0000000011086070	Spinning	Yes
Diffractometer Number	0	Measurement Temperature (°C)	25.00
Monochromatisation	None	Specimen Length	10 mm (nominal)
Divergence Slit (°)	Fixed, 0,4354	Measurement step axis	None
PSD Length (2θ)	3.32	Sample Holder	Low-background holder
Offset (2θ)	0.0000	Raw Data Origin	XRD measurement (*.XRDML)

3.3.4 Polarised Light Microscopy (PLM)

Polarised light microscopy images were obtained using a Nikon Eclipse 50i microscope (Tokyo, Japan) fitted with a Nikon DS-Fil camera and a polarised filter. The slide was placed on the stage under the 10x and 40× objective and illuminated with transmitted light. Images were taken under cross-polarised light.

3.3.5 UV/Vis analysis

A Shimadzu UV-1800 double-beam spectrophotometer (Shimadzu Corporation, Kyoto, Japan) was used for the analysis of solubility and dissolution samples. The instrument was

operated over a wavelength range of 190–1100 nm. Quartz cuvettes with a 1 cm path length were utilised for all readings.

3.3.6 Preparation of Calibration Standards

A chloroquinoline derivative stock solution was prepared by dissolving 5 mg of chloroquinoline derivative in 0.5 ml dimethyl sulfoxide (DMSO) and sonicated for about 10 minutes to establish a completely dissolved solution. Methanol was used to dilute to volume (10 ml). Further dilutions for the calibration curves were prepared in H_2O and 0.1 M HCl respectively. Calibration standards were prepared in different concentrations. In both instances curves ranging from 4 µg/ml to 25 µg/ml were prepared. Method validation followed the ICH Q2 (R1) guideline for analytical procedures (ICH Q2(R1)., 2005).

Calibration curves for the derivative in 0.1 M HCl (330 nm) and in water (266 nm) showed excellent linearity (R^2 = 0.9995 and 0.9994, respectively; Figures 3.1–3.2). Figures 3.3–3.4 overlay representative spectra of ASD vs. RM in water, highlighting the increased absorbance signal for ASD across 240–300 nm (consistent with enhanced apparent solubility) and confirming absence of interfering excipient peaks at the quantification wavelengths.

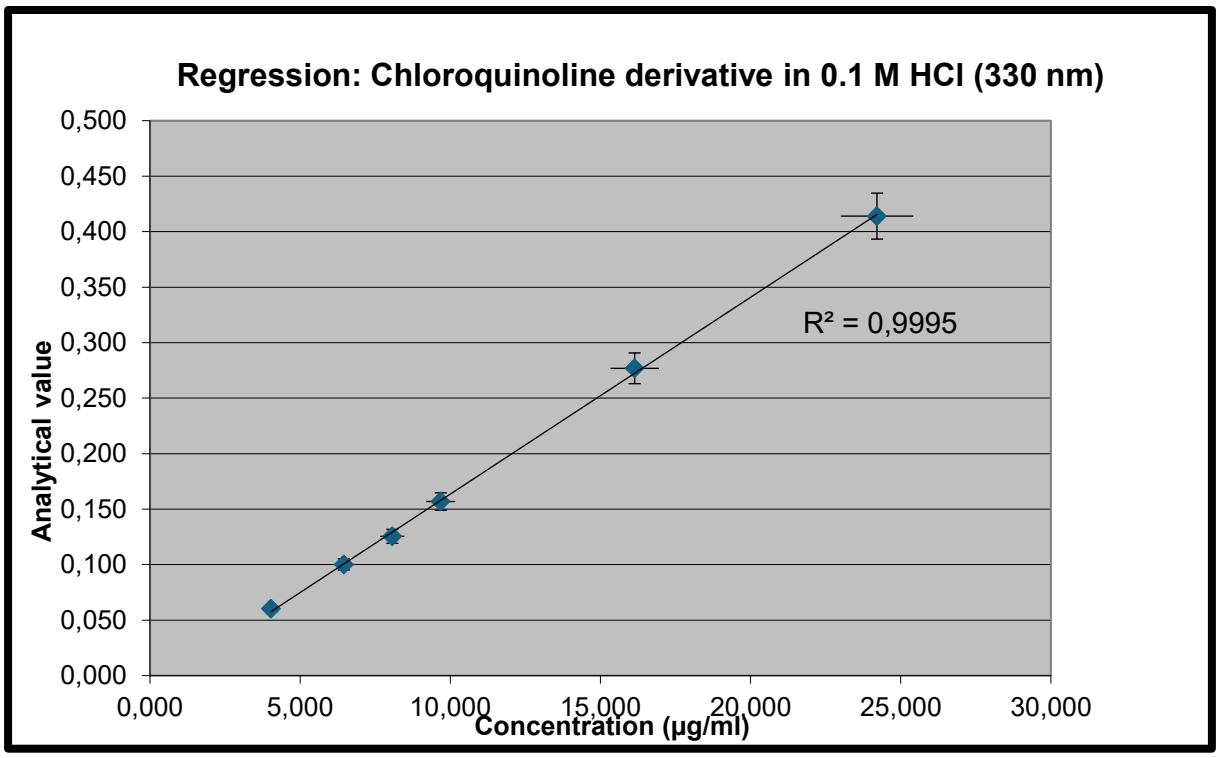

Figure 3.1: Standard curve for the chloroquinoline derivative in 0.1 M HCL at 330 nm mean ± SD (n=3).

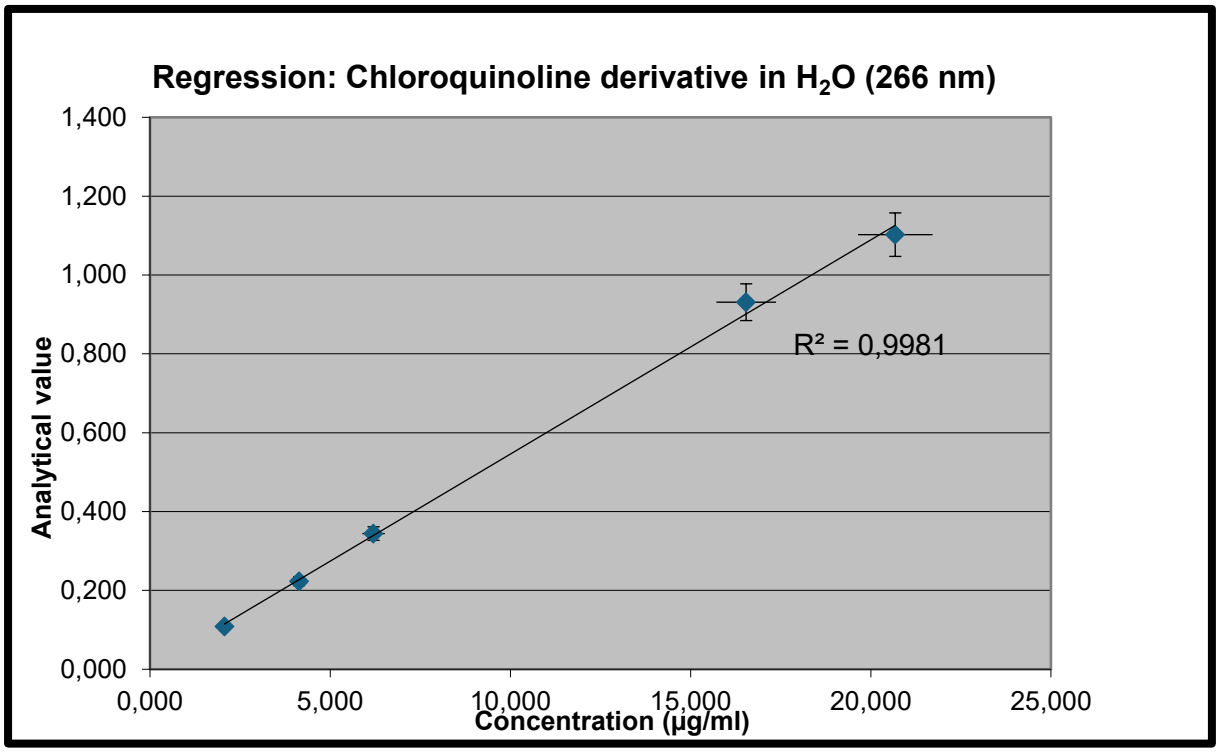

Figure 3.2: Standard curve for the chloroquinoline derivative in water at 266 nm mean ± SD (n=3).

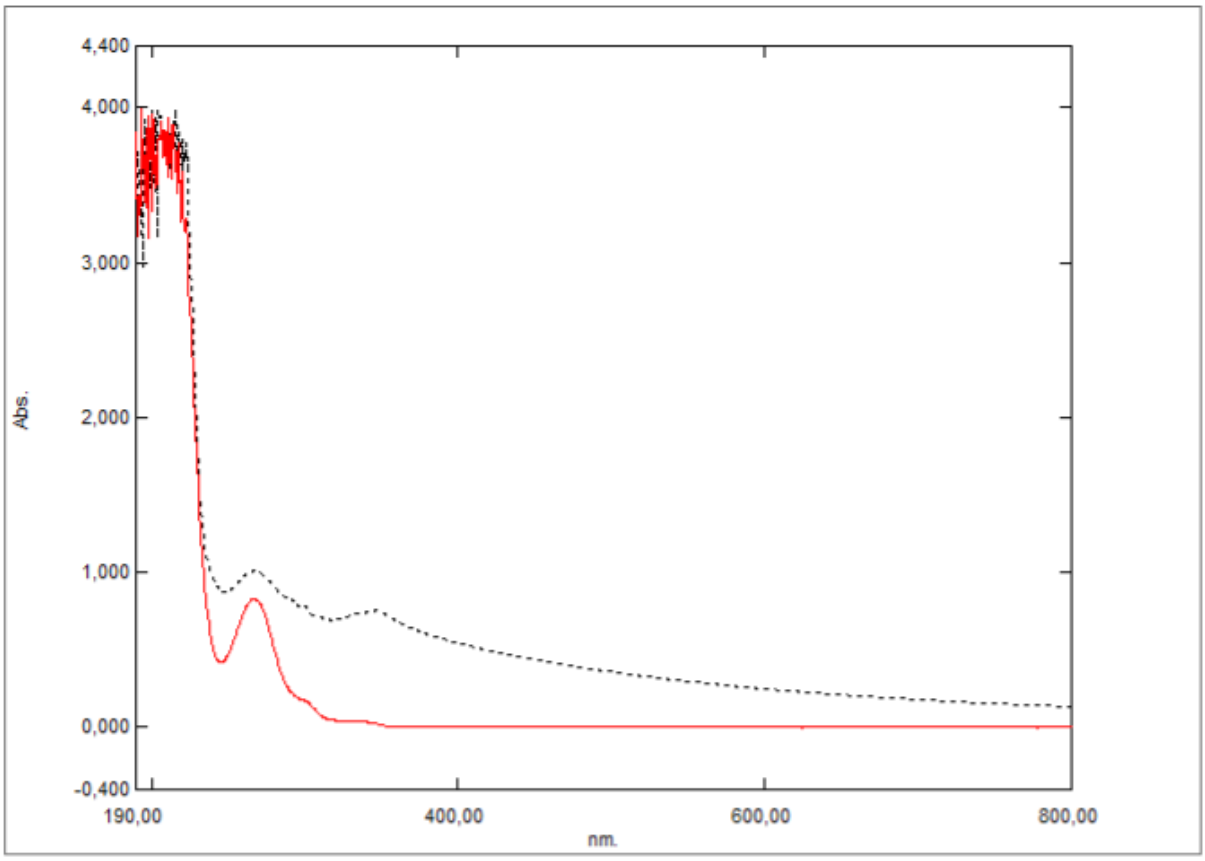

Figure 3.3: Overlay of absorbance spectra of the chloroquinoline derivative ASD (red) and raw material (black dots) in water.

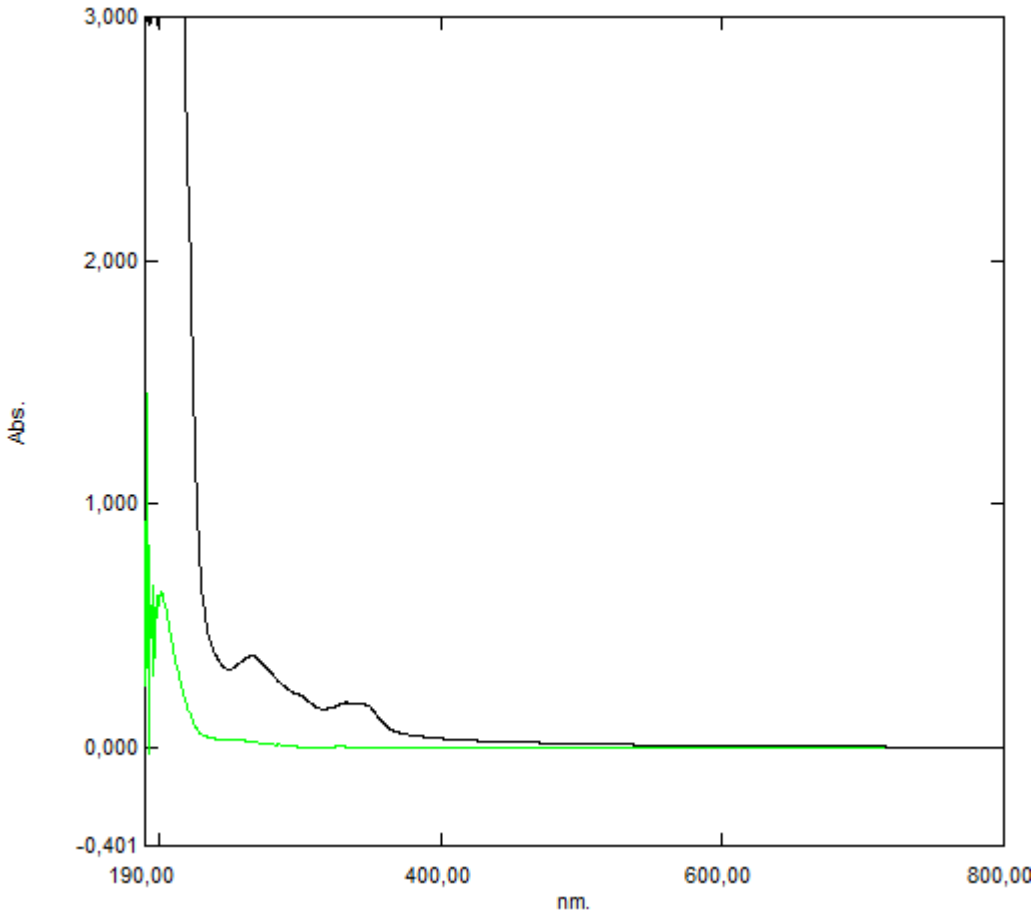

Figure 3.4: Overlay of absorbance spectra of the chloroquinoline derivative ASD (black) and raw material (green) in water.

3.3.7 Solubility Studies

Each solubility sample (10 mg), equivalent to 2 mg of chloroquinoline derivative was placed in 50 mL of distilled water using the rotating flask method. The samples were then sealed in tubes and rotated using fittings on a JULABO ED rotating water bath at 54 rpm maintained at 37°C to simulate body temperature. The solubility experiments were performed in triplicate. After 24 hours, the solutions were filtered using a 0.45 µm nylon syringe filter for analysis via UV spectrophotometry, and the absorbance of each sample was measured.

3.3.8 Dissolution Studies

A VanKel700 (Varian, Palo Alto, USA) dissolution bath equipped with USP Dissolution Apparatus 2 (paddle method) was used to evaluate the dissolution rates of the chloroquinoline derivative in both its pure and ASD formulations. The dissolution system was equipped with six separate dissolution vessels, with three used for the raw material and three for the ASD samples. Each sample (10 mg chloroquinoline derivative and 40 mg ASD) was introduced into 500 mL of distilled water and the dissolution medium was

maintained at approximately 37°C with paddle speed set at 100 rpm for 24 hours. Samples were withdrawn at 10, 20, 30 min, and 1, 2, 4 and 24 hours. A second dissolution test was conducted to assess ASD performance in acidic mediums using a 500 mL 0.1 M HCl buffer medium in all dissolution vessels at the same conditions as for the first test. Samples were analysed using UV spectrophotometry.

Results and Discussion

3.4 Preliminary development and methodology

Preceding ASD development, some unique challenges became apparent early during the planning stage of the formulation. The quantity of compound that was available to work with was limited due to its novelty and sourcing from collaborators. Further to this, its novelty meant that analytical method development and validation became a tedious process that would require high quantities of pure compound. Moreover, the raw material was completely insoluble in all available solvents with the exception of DMSO. This implied that caution as well as precise planning had to be employed during the selection of an appropriate polymer and polymer ratio and following this, limited quantities of raw compound and ASD had to be used for testing and analysis to ensure adequate amounts of the compound was available for any later experiments. Therefore, methods used were tailored with these challenges in mind.

3.4.1 Miscibility testing

This test was conducted to determine if a *T*g can be observed and whether crystallisation occurs upon heating. The absence of a melting point in the second run, could indicate miscibility. Figure 3.5 illustrates an overlay of the DSC thermograms of the API and PVP K25. Figure 3.6 shows the DSC thermograms for the 1:4 API:PVP K25 physical mixture (miscibility test).

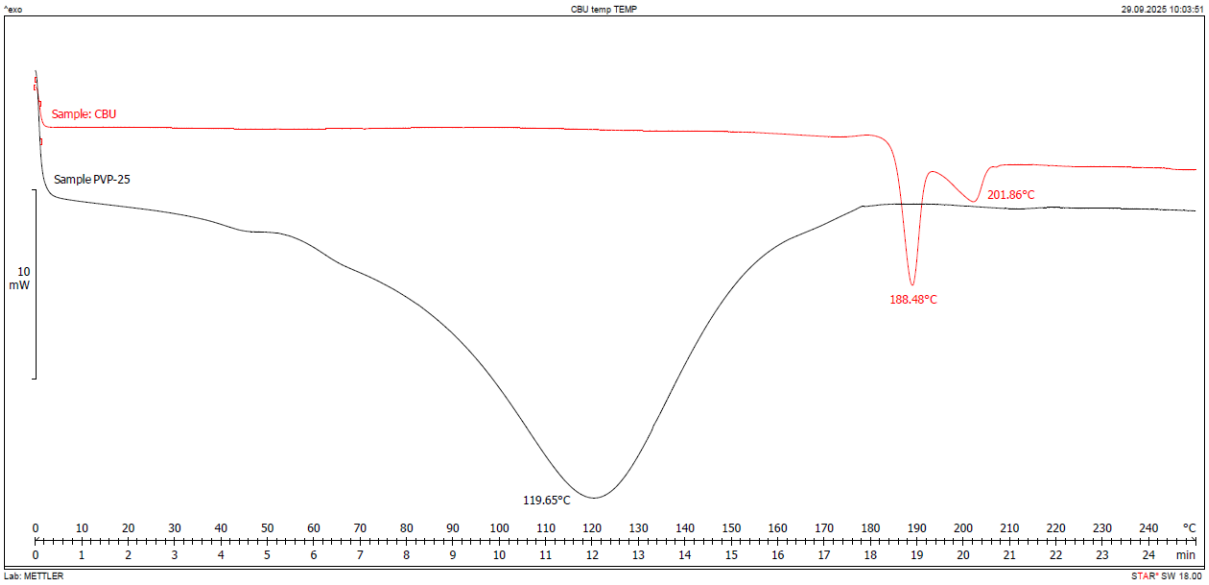

Figure 3.5: An overlay of the DSC thermograms of chloroquinoline derivative (blue) and PVP K25 (red).

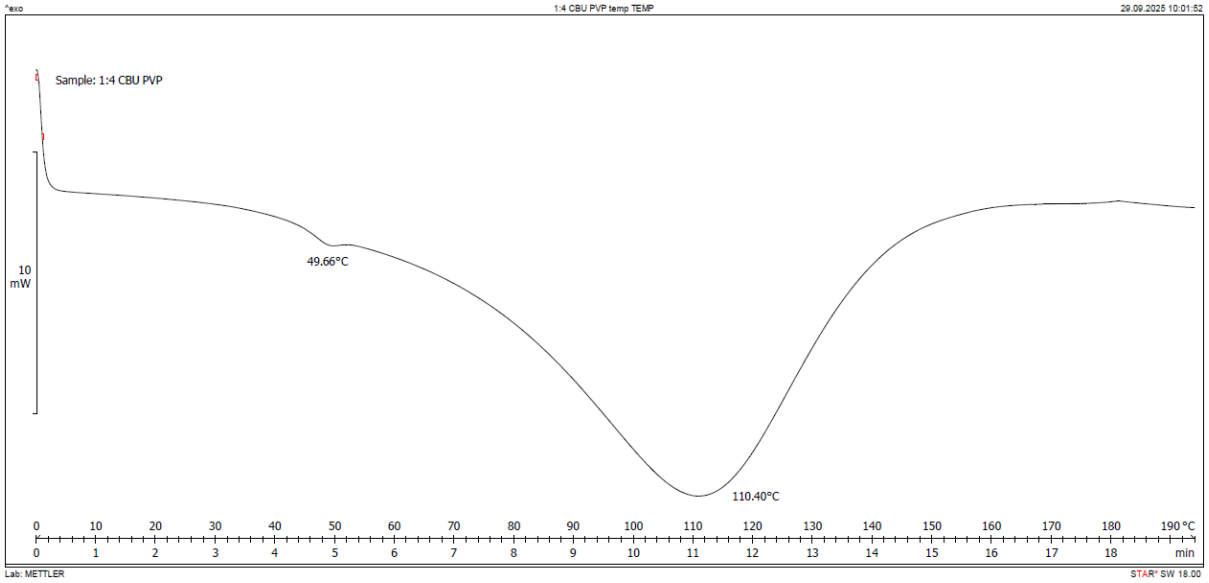

Figure 3.6: An overlay of the DSC thermograms of the miscibility test of the physical mixture of the API and PVP K25 (1:4).

The bottom thermogram represents the first thermal run, and the top thermogram the second thermal cycle. The total absence of the chloroquinoline derivative thermogram in the second run with no thermal events, indicates a miscible system. On first heating of the 1:4 physical mixture, the endotherm attributable to the drug begins to develop while the PVP K25 baseline remains featureless below its *T*g. On second heating, the drug-related endotherm is not observed within the truncated temperature range of this run; however, because these runs ended at ~190 °C, which is below the drug's melting region, the absence of a melt peak cannot, on its own, evidence miscibility. We therefore do not claim miscibility from Figures 4.5–4.6. Instead, we rely on the single-*T*g criterion observed for

the formulated ASD (water-loss DSC and mDSC; see Figures 3.9-3.10), supported by Gordon-Taylor prediction, to infer intimate mixing at 1:4 (Iyer et al., 2021; Pöstges et al., 2022).

The DSC thermograms of the raw materials (Figure 3.5) and the 1:4 API:PVP K25 physical mixture (Figure 3.6) were acquired under a programmed temperature ramp (10 °C min^{-1}) on the Mettler system described in 3.3.1, not under isothermal conditions.

In the first heating of the neat materials, the API displays a sharp endotherm at high temperature consistent with melting, while PVP K25 is featureless below its high *T*g, as expected for an amorphous polymer. For the 1:4 physical mixture (Figure 3.6), the first run shows a broadened, depressed endotherm relative to the neat API, indicating drug–polymer interactions. On the second run of the mixture, an API melt is not observed within the truncated run window; however, given the 10 °C min^{-1} program and the stop of these specific runs near ~19–25 min (≈ 190–250 °C equivalent), the absence of an endotherm in the second cycle cannot, on its own, evidence miscibility, because the program terminates at or just below the API's melting region for these runs. We therefore do not conclude "miscibility" from Figure 3.6 alone.

Instead, the miscibility inference for the formulated system is based on orthogonal evidence: after moisture removal, the "water-loss" DSC shows a single step change at ~137–142 °C assignable to the dispersion *T*g with no mass loss in that region, which is corroborated by TGA and aligns with the Gordon-Taylor prediction for the 1:4 composition. This single-*T*g criterion, together with the qualitative depression/broadening of the API endotherm in the mixture's first run, supports intimate mixing in the ASD, while avoiding over-interpretation of the second-run mixture trace where the temperature ceiling precludes a definitive melt assessment.

3.4.2 Simultaneous Thermogravimetric Analysis (STA)

A comparison of the 1:1 and 1:4 physical mixtures of the raw material with PVP K25 (Figure 3.7) revealed that the higher polymer loading (1:4) induced a more pronounced melting point depression and broader endothermic peak in the DSC thermograms relative to the lower-polymer 1:1 mixture. This behaviour suggests enhanced drug–polymer interactions at the increased polymer content, which shows that greater melt depression serves as an indicator of potential amorphous-phase stability and improved glass-forming ability. Furthermore, PVP K25 itself features a relatively high glass-transition temperature, supporting the formation and maintenance of an amorphous matrix that can retard crystallisation. The 1:4 ratio was selected for ASD formulation to maximize these benefits ensuring sufficient polymer presence to stabilize the drug in its amorphous state. These

observations also provide the basis for deeper investigation by complementary analytical techniques to further validate the physical stability and suitability of this drug-polymer system for ASD development.

The STA traces were acquired under a linear heating program of 10 °C·min^{-1}. The neat API shows a narrow, high-temperature endotherm attributable to melting. By contrast, the 1:1 and 1:4 API:PVP K25 mixtures present a wide, shallow endothermic region in the same thermal domain. This broad response is consistent with overlapping thermal events when crystalline API is in contact with the polymer, namely depression of the fusion onset (eutectic-like behaviour) together with progressive dissolution of molten API into a softening polymer matrix. The absence of a concomitant exotherm argues against recrystallisation in this window.

These runs terminate at ~19 min (≈ 190 °C), i.e., before the full melting interval of the API is traversed. Consequently, while broadening and reduced peak intensity qualitatively indicate polymer-perturbed fusion, a numerical melting-point depression (ΔTm) cannot be substantiated from Figure 3.7 alone. No ΔTm is therefore reported here. Evidence for intimate mixing in the formulated ASD is instead drawn from orthogonal data, specifically, a single glass-transition step after water loss in DSC/mDSC (~137–142 °C) in agreement with the Gordon-Taylor estimate for the 1:4 composition (Baird & Taylor, 2012).

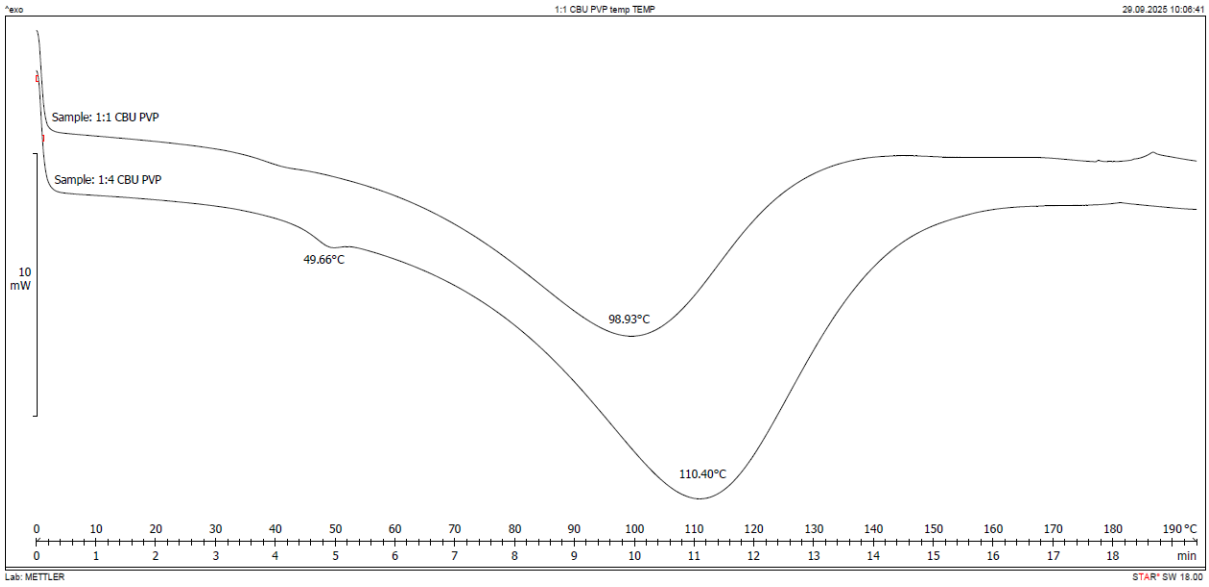

Figure 3.7: Showing DSC thermograms of physical mixtures for 1:1 chloroquinoline derivative and PVP K25 (red) and 1:4 chloroquinoline derivative and PVP K25 (black).

Upon development of the formulation via solvent evaporation with PVP K25, the DSC traces of the ASD were re-examined to look at two specific features: complete amorphisation of the drug-polymer combination post formulation through the creation of a single distinct *T*g shift and the extent of this transition with regards to the temperature it would be seen thus giving a rough indication of the apparent stability of the ASD from literature.

Figure 3.8 shows a broad sub-Tm endothermic region in the blend/ASD. Because the second-heat terminates before the API's full melt, this feature is attributed to polymer relaxation/enthalpic recovery and progressive solid-state mixing/dissolution of drug into the polymer, not to melting-point depression during initial heating, followed by a much later step-wise temperature shift at 138.11°C. In principle, initial observations went against the theory of well-formed ASDs exhibiting singular *T*g events. The appearance of multiple transitions in the sample suggested potential factors such as residual moisture, partial phase separation, or incomplete miscibility. Notably, this was unexpected given that the earlier physical mixture data had indicated a stable drug-polymer system. To explore the possibility of water or DCM contributing to these additional transitions a further investigation was warranted by performing a DSC analysis incorporating a water-loss step. This aimed to remove residual moisture and thereby clarify whether the anomalous events were genuinely linked to sample heterogeneity or simply a result of water plasticising the system.

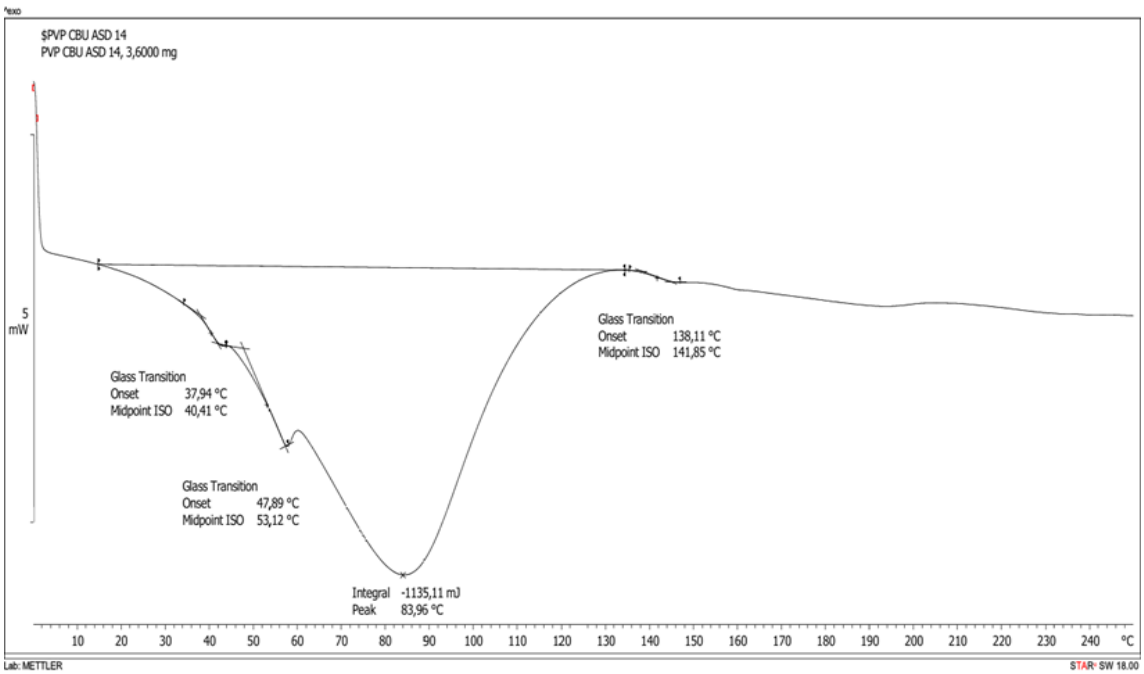

Figure 3.8: First DSC thermogram obtained for chloroquinoline derivative 1:4 ASD.

The water loss DSC thermogram (Figure 3.9) of the 1:4 the chloroquinoline derivative ASD illustrates several thermal events that are significant for understanding the thermal profile

of the formulation through the use of both heating and cooling phases. The DSC curve exhibited prominent endothermic peaks between 40°C and 70°C during the first heating cycle with a third peak observed at 66.34°C. The ASD was rapidly cooled thereafter at 100°C, causing a repetition of the peaks observed during the first heating cycle but a loss in the peak at 66.34°C. During the third heating cycle, the peaks between 40 and 70°C were mirrored and the sample was run till eventually a stepwise transition was observed much later at 136.98°C almost similar to what was observed in an earlier thermogram.

The second-heat Tg (~140–144 °C) coincides with literature values for PVP K25, indicating a polymer-rich matrix response. This Tg does not by itself prove complete miscibility; we therefore compare the measured Tg with the Gordon-Taylor prediction and interpret the solid-state structure using XRPD (halo) and PLM together.

The observation of this later stepwise change in temperature represents one consistency which was noted for this ASD and is almost consistent with the *T*g observed in literature for PVP K25 at approximately 160°C. The *T*g of the raw material was not fully observable during testing however it was found that at extremely high temperatures it did not thermally degrade as observed in the TGA analysis as well as during all DSC runs up to 200°C which aligns with the possibility of a high *T*g found in compounds with this feature. The loss of the endothermic peak around 66.34°C during rapid cooling can be largely attributed to a loss in moisture, further supported by the TGA (Figure 3.9) losing 4.24% or 0.21 mg of total mass from the 5 mg sample tested around the boiling point temperature of water and thereafter no thermal degradation was noted through a loss in mass during the run window.

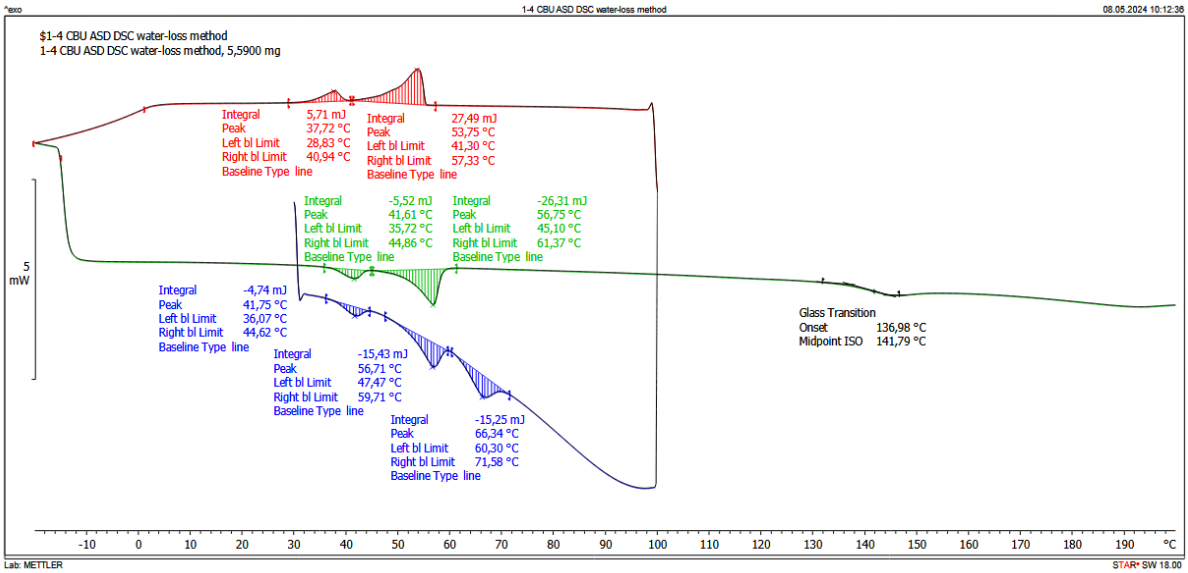

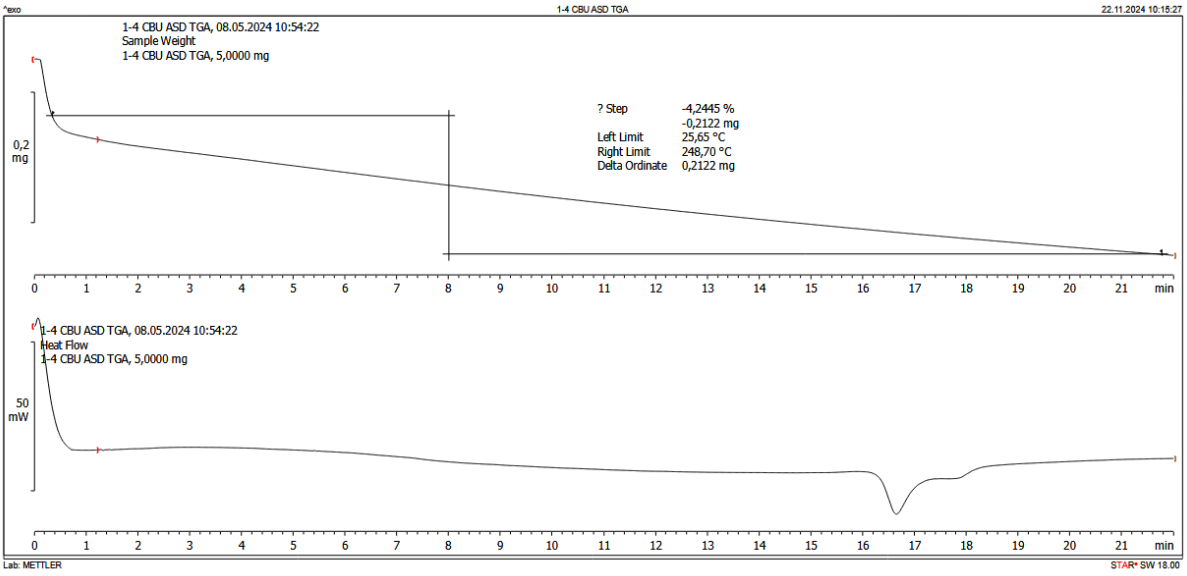

Figure 3.9: Showing DSC thermogram with water loss method (top) and corresponding TGA analysis (bottom).

To further validate the observed temperature for *T*g the Gordon-Taylor equation (eq 4.1) for a binary ASD system may be used (Krummnow et al., 2023). *T*g is estimated here on the basis of the weight fractions of each component and their respective *T*g values.

$$Tg = (w1Tg1 + kw2Tg2)/(w1 + kw2) \qquad \text{Equation (4.1)}$$

From the Gordon-Taylor equation the predicted *T*g value was found to be 141.6°C using a combination of data from literature for PVP K25, known *T*gs for both materials and weight fractions. Due to limitations in raw material quantities, k was assumed on the basis of volume additivity as 1. This value deviated positively from observed values by 4.6°C. Minor differences in temperature observed from Figure 4.9 may be influenced by factors such as intermolecular interactions between the drug and polymer or even the oversimplification of k where a more accurate estimation may be derived from density data obtained for both materials.

Consequently, an observation that went unanswered from current data was the double peak phenomenon that remained during both heating cycles and was therefore further investigated through MDSC.

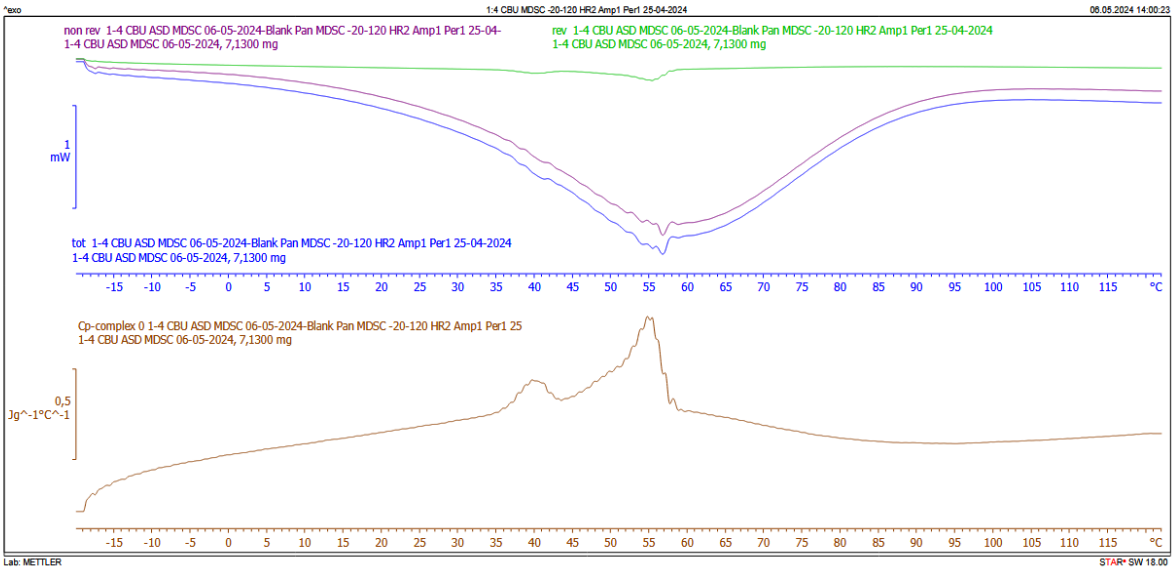

Figure 3.10: Showing the MDSC analysis for 1:4 chloroquinoline derivative ASD.

In Figure 3.10, the reversing heat flow signal showed a subtle baseline shift around 55°C typical of a *T*g seen in this heat flow signal, while the non-reversing signal reveals a broad endotherm consistent with gradual moisture loss or enthalpic relaxation of the newly formed amorphous matrix at around the same temperature. The Cp-complex trace reflected the baselines shift seen in the reversing heat flow signal with a similar change in baseline. This observation, in tandem with the split between the reversing and non-reversing heat flows, implies that the event could represent either a secondary *T*g (e.g., a sub *T*g relaxation process) or a localised relaxation phenomenon within the amorphous matrix. Indeed, the previous water loss DSC experiments and TGA measurements revealed approximately 4–5% mass loss due to moisture, which can plasticize the polymer and shift or broaden thermal transitions. While this process could occur within the system and shift or broaden the observed transitions, moisture is not necessarily the sole driver of the repeated peaks. Once the majority of free water is removed, the non-reversing heat flow may still capture enthalpic relaxation or polymer-drug interactions that release energy over a broad temperature range. Moreover, if the polymer has an intrinsic secondary relaxation near 40–60 °C, this can persist independently of moisture. Taken together, these findings underscore that multiple factors such as residual bound water, sub-*T*g relaxations, and potential minor phase separations could contribute to the transitions in this region. This aligns with the notion that the amorphous system can have more than one mobility regime and provides a basis for further explorations into the physical stability and relaxation dynamics of the formulation.

3.4.3 X-ray Powder Diffraction (XRPD) Analysis

Figure 4.11 depicts the diffractogram for raw chloroquinoline derivative with several sharp peaks observed at 2θ positions 11.36°, 13.02°, 15.28°, 17.38°, 17.73°, 18.90°, 21.01°, 22.04°, 22.24°, 22.5°, 23.72°, 25.26°, 25.43°, 26.97°, 27.52° and 28.68° with the highest intensity at 23.72° corresponding to a relative intensity of 100% and a full width at half-maximum (FWHM) of 0.1653°. The high incidence of Bragg peaks at the aforementioned 2θ positions coupled with their high intensities indicates a considerable degree of crystallinity, ordered molecular arrangement and therefore tight molecular packing and low ΔG akin to typical crystalline molecular structures.

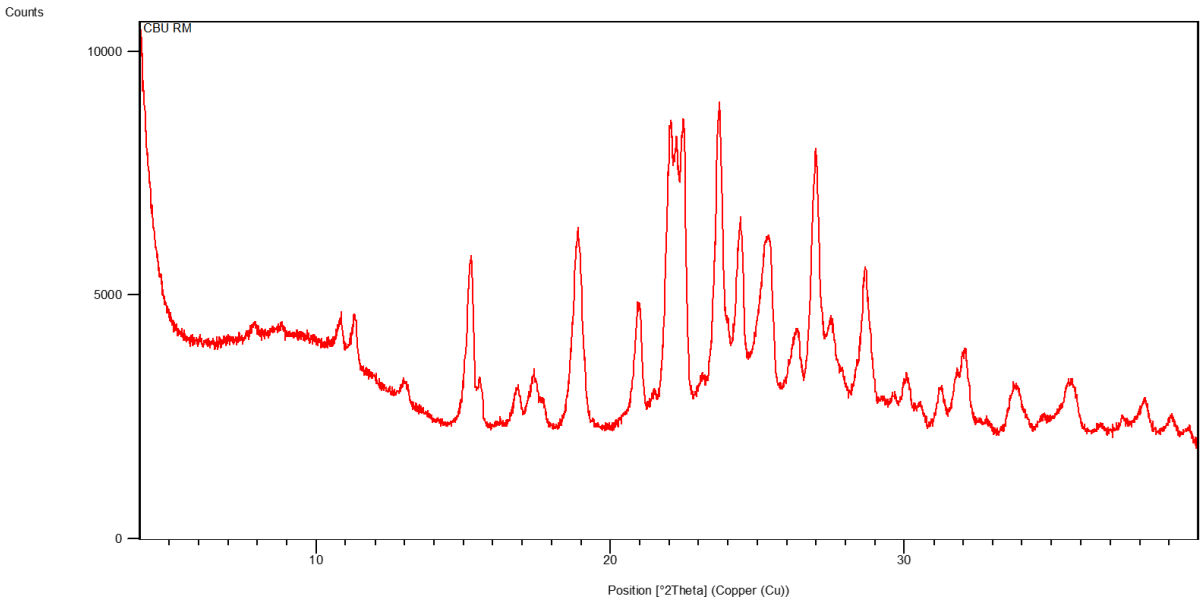

Figure 3.11: XRD diffractogram of chloroquinoline derivative raw material y-axis = relative intensity (%) and x-axis = position (2θ).

The narrow FWHM value further underscores the rigid packing of molecules in the crystalline lattice which further illustrated potential challenges for dissolution and bioavailability in this compound.

Inversely, Figure 3.12 showed no sharp peaks of high intensity with possible exceptions at the 11° and 15° 2θ positions. The total crystallinity content for this ASD can be calculated by using % crystallinity equation (Duddu et al., 2020):

$$\%Crystallinity = \frac{\text{Area of Crystalline Peaks}}{\text{Total Area (Crystalline+Amorphous)}} \times 100 \qquad \text{Equation (4.2)}$$

This value was calculated as 14,99% using observable obtained peak heights indicating partial crystallinity with the ASD remaining moderately amorphous representing a modest reduction in overall crystalline features. The XRPD analysis provided evidence of slight crystallinity within the ASD, which correlates with the exothermic events seen in the DSC analysis. The partial crystallinity however does remain a concern for the viability of the ASD and this largely may be attributed to the inherent insolubility of the raw material even when combined with a water-soluble polymer such as PVP-K25. The use of a solvent-based technique is therefore limited in this aspect in the pursuit of creating a fully amorphous ASD, however, it has proven that creating ASDs is possible even with a raw material that proved difficult to handle in the given circumstances and conditions with some consequential drawbacks on crystallinity.

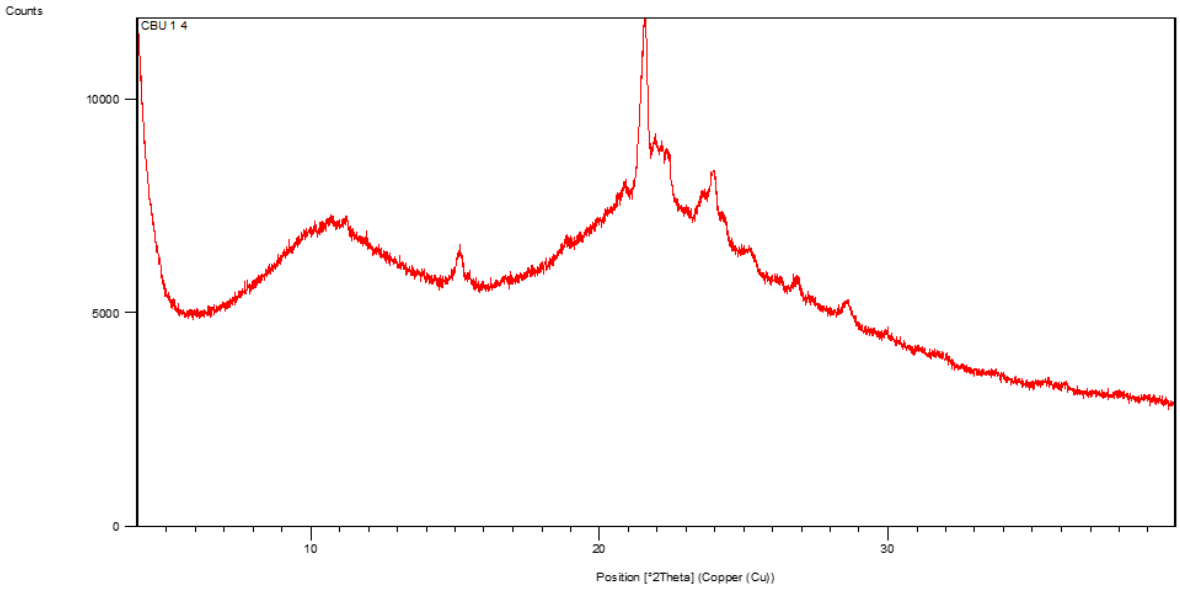

Figure 3.12: XRPD diffractogram of the 1:4 ASD y-axis = Relative intensity (%) and x-axis = Position (2θ).

Additional exploration into whether the ASD will be feasible during solubility and dissolution testing may further validate the future use of techniques using solvents but with more optimisation on certain formulation elements such as solvent matrix used, mixing times or additional polymer selection studies in order to achieve an ASD ideally with 0% crystallinity.

Although a small apparent shift in one of the dominant Bragg reflections can be seen when comparing Figure 3.11 and Figure 3.12, the low intensity of the remaining peaks in the ASD and the limited quantity of material available did not permit a dedicated study of potential new crystalline forms. This possibility is therefore acknowledged as a limitation of the current work and recommended for future investigation.

3.4.4 Polarised Light Microscopy (PLM)

The PLM images of the ASD (Figure 3.13) showed distinct morphology compared to the pure material (Figure 3.14). For the ASD, the images reveal a less crystalline structure with scattered, irregular aggregates, indicative of disrupted crystal lattice formation. With supporting evidence from the XRD analysis, this aligns the indication of almost complete amorphisation and partial crystallinity. The regions of slight colour refraction under high magnification of 100 µm (highlighted with red arrows) suggests areas of significant birefringence.

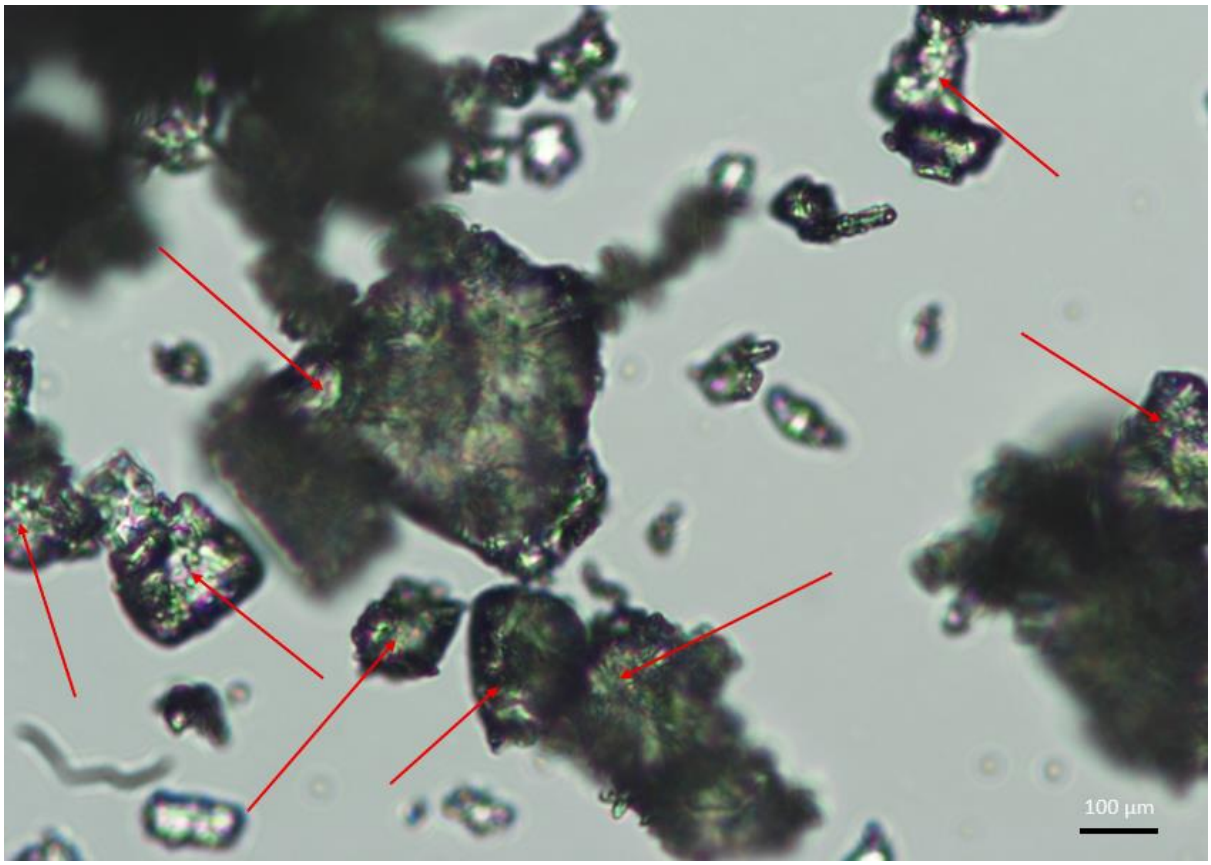

Figure 3.13: PLM image of 1:4 ASD.

In contrast, the chloroquinoline derivative images exhibit a characteristic birefringence under polarised light with bright spots visible under low magnification (200 µm). This can be seen in Figure 3.14 in areas circled in red where bright spots of material appear essentially where particles of powder were refracting large quantities of polarised light supporting earlier XRPD data where high crystallinity can be observed.

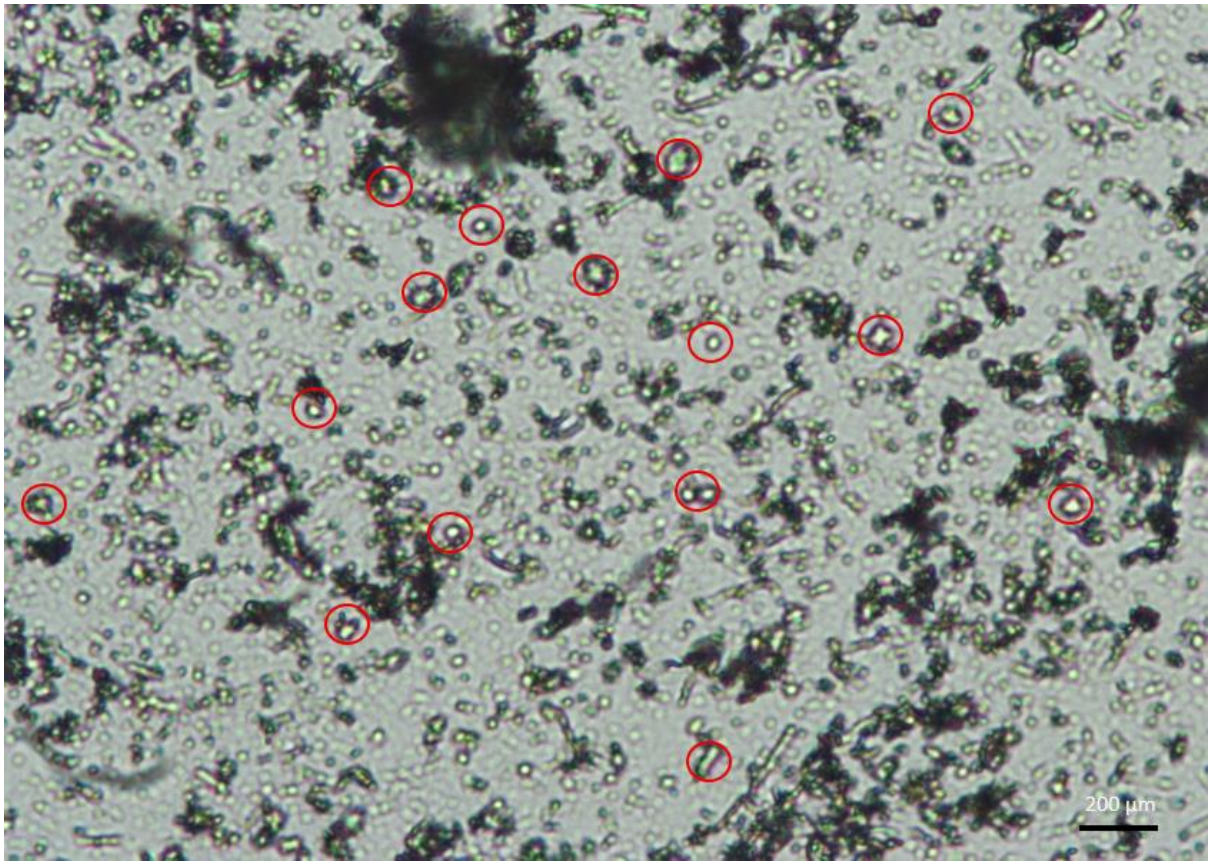

Figure 3.14: PLM image of raw material.

This together with complementary data from earlier analyses supports the indication of effective, though incomplete, dispersion of the chloroquinoline derivative in the polymer matrix and thus limiting its ability to recrystallise (Gao et al., 2023).

3.5 Solubility Study

Before progressing with dissolution studies, a preliminary test of the formulation's solubility capacity was conducted to better access its predicted performance. This also would serve as an informative backbone as to whether the ASD would possibly require reformulation going forward. From the results in Figure 3.15, the ASD formulation had a profound enhancement in solubility when compared to the pure material, which had negligible solubility under identical conditions.

The observed solubility enhancement across all the three chloroquinoline derivative ASD samples containing PVP K25 in a 1:4 ratio therefore suggests potential success in having an improved dissolution profile in further testing. In contrast, the pure compound's insolubility was further demonstrated as it was unable to be detected at any validated peak wavelengths and registered null ratings throughout in water highlighting its complete inability to dissolve in aqueous mediums.

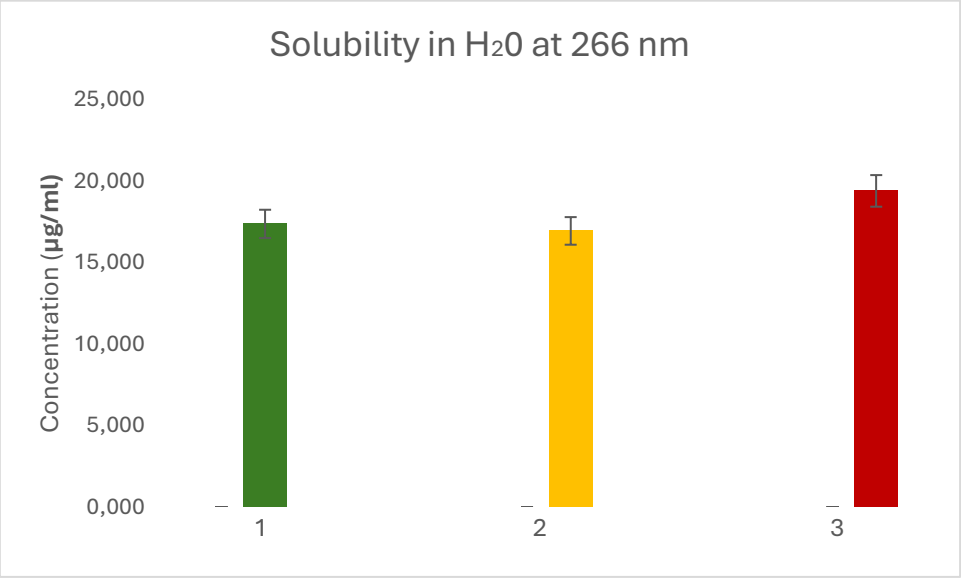

Figure 3.15: Bar graph showing preliminary solubility results for pure compound vs 1:4 ASD. Green = Raw material vs ASD sample 1; Yellow = Raw material vs ASD sample 2; Red = Raw material vs ASD sample 3 data are mean ± SD (n = 3)

Overall, these findings confirm that the preparation of the chloroquinoline derivative as an ASD with PVP significantly enhances its solubility therapeutic potential (solubility values: CBU vs ASD sample 1 17.37 µg/ml vs 0 for raw material; CBU vs ASD sample 2 16.94 µg/ml vs 0,01 for raw material; CBU vs ASD sample 3 19.40 µg/ml vs 0 for raw material) Future work could further explore the optimisation of polymer ratios and processing conditions to refine the solubility and stability profile of the ASD formulations.

3.6 Dissolution Study

In water at 266 nm (Figure 3.16), the ASD exhibited a marked improvement in dissolution rates compared to the pure compound which was reflected earlier in improved solubility rates during solubility studies. This can be attributed to the amorphous state of the chloroquinoline derivative in the ASD, facilitated by the polymer matrix, which disrupts the crystalline lattice and promotes molecular dispersion. The choice of PVP K25, a hydrophilic polymer known for stabilising amorphous states and enhancing wettability, underscores the formulation's ability to overcome solubility barriers. An initial spring effect of drug dissolution may be observed from initial rapid drug dissolution at 10 minutes followed by a broad plateau to ~4 h and then a gradual secondary increase after ~8 h, reaching ~60% at 24 h. Because the profile does not decline, a ‘parachute’ effect is not observed (Schittny et al., 2020). The late-stage increase (> 8 h) is most consistent with slow polymer hydration and erosion-controlled release of drug-rich domains, together with progressive wetting of residual crystalline particles seen by PLM/XRPD (Meng et al., 2021; Schittny et al., 2020).

In pure water the absence of a downward trend suggests the solution never exceeded an apparent solubility threshold that would drive re-precipitation instead, dissolution continued slowly as the PVP matrix hydrated and as particle surface area increased due to fragmentation. Interestingly, the drug demonstrated an elevation in dissolution at 24 h suggesting that there is potential for further dissolution tests to be prepared for elongated instances past the 24-hour window to better observe any inherent extended-release characteristics within the formulation. The dissolution results for the ASD in water after 24 h were determined as 59.76%, in comparison to the 10.07% of the raw material (Figure 3.16).

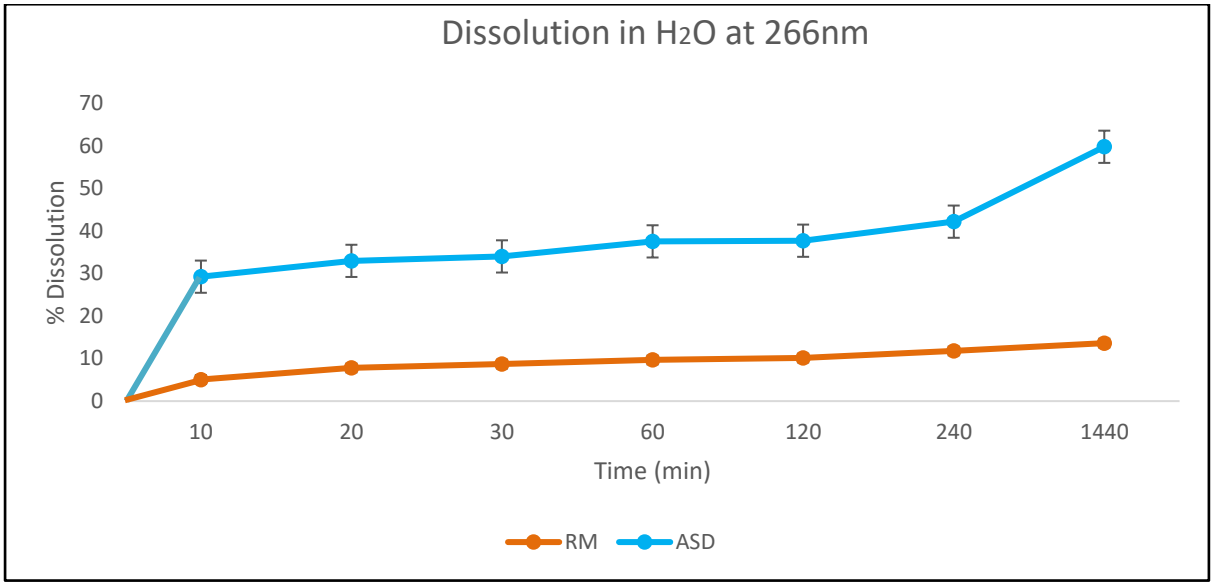

Figure 3.16: Dissolution study conducted in water at 266 nm for ASD (blue) and raw material (orange) (USP Apparatus II, 50 rpm, 37 ± 0.5 °C). Time in minutes; data are mean ± SD (n = 3).

Similarly, results were taken from a second validated UV wavelength to ensure robustness and reliability from obtained results, at 333 nm (Figure 3.17). The dissolution characteristics of pure compound and ASD was assessed in acidic media of 0.1 N HCl (pH 1.2) in this instance to look at the effect of low pH environments such as those found within the gastrointestinal tract. These results demonstrated that the effects of pH were largely negligible and similar to those of water on the solubility characteristics of the chloroquinoline derivative where a similar spring parachute effect was observed. This can be further demonstrated by using the similarity factor (*f*2) which is a comparative analysis equation used by regulatory authorities to determine the alignment of dissolution profiles against each other and often proves to be more accurate than using T-tests (Pereira et al., 2025).

$$f2 = 50.\log\left[(1 + \frac{1}{n}\sum_{n=1}^{n}(\mathrm{Rt} - \mathrm{Tt})^2)^{-0.5}).100\right] \quad \text{(Equation 4.3)}$$

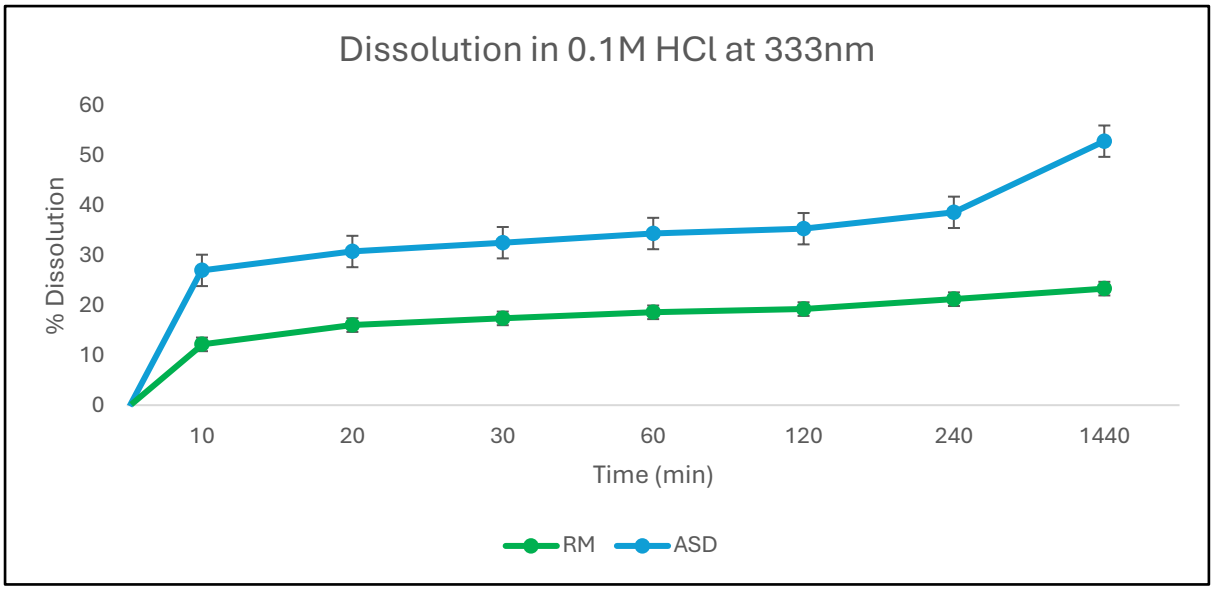

Figure 3.17: Dissolution study conducted in 0.1 N HCl at 333 nm for ASD (purple) and raw material (green) (USP Apparatus II, 50 rpm, 37 ± 0.5 °C). Time in minutes; data are mean ± SD (n = 3).

Where Rt is reference % dissolution, Tt: Test % dissolution and n are the number of time points. The calculated f_2 was 88.64 (where 100 is identical), indicating a high degree of similarity between the ASD's dissolution in water and in acid.

Additionally, the Pearson's correlation coefficient can be applied to the data set and was found to have a value of 0.9979 further showing the strong positive correlation with the profiles. This suggests that the acidic environment does not negatively affect or greatly change the dissolution profile of the compound or its ASD, thereby validating the robustness of the formulation against pH variations in the gastrointestinal tract. Such stability is impactful for ensuring acceptable therapeutic performance in specific physiological conditions and potential extension of the studies towards more stringent *in vitro* dissolution setups like USP apparatus IV where *in vivo* conditions are more closely mimicked, *in vivo* studies in animal models or a wider range of pH media.

The dissolution results for the ASD in 0.1 N HCL after 24 h was determined as 52.77%, in comparison to the 9.89% of the raw material (Figure 3.17).

3.7 Conclusion

The formulation of the chloroquinoline-benzothiazole-urea compound as a PVP K25-based ASD resulted in improved solubility and dissolution compared to the crystalline drug. Characterization techniques confirmed partial amorphisation, with XRPD indicating ~15% residual crystallinity. Thermal analysis showed a single *T*g temperature (~137 °C) close to the Gordon-Taylor predicted value (141.6 °C), supporting miscibility. The ASD demonstrated a six-fold increase in solubility (up to 19.4 µg/mL) and markedly enhanced dissolution in both water (59.76%) and acidic media (52.77%) after 24 hours. Dissolution profiles were highly similar (f_2 = 88.64), indicating robust, pH-independent release. These results confirm that ASD formulation is a viable strategy for improving the aqueous performance of this poorly soluble compound, however, further improvements in formulation technique and even wider polymer selection will allow for the creation of a more ideal ASD for future testing.

Reference List

Asgreen, C., Knopp, M. M., Skytte, J., & Löbmann, K. (2020). Influence of the polymer glass transition temperature and molecular weight on drug amorphization kinetics using ball milling. *Pharmaceutics*, *12*(6). https://doi.org/10.3390/PHARMACEUTICS12060483

Aulifa, D. L., Al Shofwan, A. A., Megantara, S., Fakih, T. M., & Budiman, A. (2024). Elucidation of Molecular Interactions Between Drug & Polymer in Amorphous Solid Dispersion by a Computational Approach Using Molecular Dynamics Simulations. *Advances and Applications in Bioinformatics and Chemistry*, *17*, 1–19. https://doi.org/10.2147/AABC.S441628

Baird, J.A. & Taylor, L.S. (2012). Evaluation of amorphous solid dispersion properties using thermal analysis. Advanced Drug Delivery Reviews, 64(5), 396–421. https://doi.org/10.1016/j.addr.2011.07.009

Bhujbal, S. V., Mitra, B., Jain, U., Gong, Y., Agrawal, A., Karki, S., Taylor, L. S., Kumar, S., & (Tony) Zhou, Q. (2021). Pharmaceutical amorphous solid dispersion: A review of manufacturing strategies. *Acta Pharmaceutica Sinica B*, *11*(8), 2505–2536. https://doi.org/10.1016/J.APSB.2021.05.014

Budiman, A., Handini, A. L., Muslimah, M. N., Nurani, N. V., Laelasari, E., Kurniawansyah, I. S., & Aulifa, D. L. (2023). Amorphous Solid Dispersion as Drug Delivery Vehicles in Cancer. *Polymers 2023, Vol. 15, 3380*, *15*(16), 3380. https://doi.org/10.3390/POLYM15163380

Chen, Y., Liu, C., Chen, Z., Su, C., Hageman, M., Hussain, M., Haskell, R., Stefanski, K., & Qian, F. (2015). Drug-polymer-water interaction and its implication for the dissolution performance of amorphous solid dispersions. *Molecular Pharmaceutics*, *12*(2), 576–589. https://doi.org/10.1021/MP500660M

Craig, D. Q. M. (2002). The mechanisms of drug release from solid dispersions in water-soluble polymers. International Journal of Pharmaceutics, 231(2), 131–144. https://doi.org/10.1016/S0378-5173(01)00891-2

Dereymaker, A., & Van Den Mooter, G. (2015). The peculiar behavior of the glass transition temperature of amorphous drug-polymer films coated on inert sugar spheres. *Journal of Pharmaceutical Sciences*, *104*(5), 1759–1766. https://doi.org/10.1002/JPS.24395

Dohrn, S., Luebbert, C., Lehmkemper, K., Kyerematen, S. O., Degenhardt, M., & Sadowski, G. (2021). Solvent influence on the phase behavior and glass transition of Amorphous Solid Dispersions. *European Journal of Pharmaceutics and Biopharmaceutics*, *158*, 132–142. https://doi.org/10.1016/J.EJPB.2020.11.002

Dohrn, S., Reimer, P., Luebbert, C., Lehmkemper, K., Kyerematen, S. O., Degenhardt, M., & Sadowski, G. (2020). Thermodynamic Modeling of Solvent-Impact on Phase Separation in Amorphous Solid Dispersions during Drying. *Molecular Pharmaceutics*, *17*(7), 2721–2733. https://doi.org/10.1021/ACS.MOLPHARMACEUT.0C00418/SUPPL_FILE/MP0C00418_SI_001.PDF

DSC Analysis of Polymers | Thermal | EAG Laboratories. (n.d.). Retrieved November 1, 2024, from https://www.eag.com/app-note/characterization-of-polymers-using-differential-scanning-calorimetry-dsc/

Duddu, S. P., et al. (2020). Characterization of Amorphous Solid Dispersions and Identification of Low Levels of Crystallinity by TEM. *Molecular Pharmaceutics*, 17(12), 4693–4708.

Gao, Y., Zhao, X., Chen, Y., et al. (2023). Ternary solid dispersions: A review of the preparation, characterization, and applications. Pharmaceutics, 15(8), 2116.

Garcia-Granda, S., & Montejo-Bernardo, J. M. (2004). X-Ray Diffraction - Powder. *Encyclopedia of Analytical Science: Second Edition*, 389–397. https://doi.org/10.1016/B0-12-369397-7/00671-3

Gill, P., Moghadam, T. T., & Ranjbar, B. (2010). Differential Scanning Calorimetry Techniques: Applications in Biology and Nanoscience. *Journal of Biomolecular Techniques : JBT*, *21*(4), 167. https://pmc.ncbi.nlm.nih.gov/articles/PMC2977967/

Hajikarimi, P., & Moghadas Nejad, F. (2021). Time–temperature superposition. *Applications of Viscoelasticity*, 83–105. https://doi.org/10.1016/B978-0-12-821210-3.00006-1

Hamed, R., Mohamed, E. M., Sediri, K., Khan, M. A., & Rahman, Z. (2021). Development of stable amorphous solid dispersion and quantification of crystalline fraction of lopinavir by spectroscopic-chemometric methods. *International Journal of Pharmaceutics*, *602*, 120657. https://doi.org/10.1016/J.IJPHARM.2021.120657

Hancock, B. C., & Parks, M. (2000). What is the true solubility advantage for amorphous pharmaceuticals? *Pharmaceutical Research*, *17*(4), 397–404. https://doi.org/10.1023/A:1007516718048

Hancock, B. C., & Zografi, G. (1997). Characteristics and significance of the amorphous state in pharmaceutical systems. Journal of Pharmaceutical Sciences, 86(1), 1–12. https://doi.org/10.1021/js9601896

International Council for Harmonisation (ICH). 2005. Q2(R1): Validation of Analytical Procedures—Text and Methodology. Current Step 4 version (Q2A + Q2B combined, November 2005). Available from the ICH guideline library.

Iyer, R., Jovanovska, V. P., Berginc, K., Jaklič, M., Fabiani, F., Harlacher, C., Huzjak, T., & Sanchez-Felix, M. V. (2021). Amorphous Solid Dispersions (ASDs): The Influence of Material Properties, Manufacturing Processes and Analytical Technologies in Drug Product Development. *Pharmaceutics*, *13*(10), 1682. https://doi.org/10.3390/PHARMACEUTICS13101682

Kawakami, K., Bi, Y., Yoshihashi, Y., Sugano, K., & Terada, K. (2018). Time-dependent phase separation of amorphous solid dispersions: Implications for accelerated stability studies. *Journal of Drug Delivery Science and Technology*, *46*, 197–206. https://doi.org/10.1016/J.JDDST.2018.05.016

Kalepu, S., & Nekkanti, V. (2015). Insoluble drug delivery strategies: review of recent advances and business prospects. *Acta Pharmaceutica Sinica. B*, *5*(5), 442. https://doi.org/10.1016/J.APSB.2015.07.003

Krummnow, M., Lübbert, C., Thommes, M. & Breitkreutz, J. (2023) Thermodynamic Modeling of the Amorphous Solid Dispersion-Water Interfacial Layer and Its Impact on the Release Mechanism. Pharmaceutics, 15(5), 1539. https://doi.org/10.3390/pharmaceutics15051539

Leyva-Porras, C., Cruz-Alcantar, P., Espinosa-Solís, V., Martínez-Guerra, E., Piñón-Balderrama, C. I., Martínez, I. C., & Saavedra-Leos, M. Z. (2019). Application of Differential Scanning

Calorimetry (DSC) and Modulated Differential Scanning Calorimetry (MDSC) in Food and Drug Industries. *Polymers*, *12*(1), 5. https://doi.org/10.3390/POLYM12010005

Lemmer, H. J. R., & Liebenberg, W. (2013). *Preparation and evaluation of metastable solid-state forms of lopinavir*. Pharmazie, 68(4), 327–332. https://doi.org/10.1691/ph.2013.2194

Li, Y., A. Day, D., Stark, H., L. Jimenez, J., & Shiraiwa, M. (2020). Predictions of the glass transition temperature and viscosity of organic aerosols from volatility distributions. *Atmospheric Chemistry and Physics*, *20*(13), 8103–8122. https://doi.org/10.5194/ACP-20-8103-2020

Liu, X., Feng, X., Williams, R. O., & Zhang, F. (2018). Characterization of amorphous solid dispersions. *Journal of Pharmaceutical Investigation*, *48*(1), 19–41. https://doi.org/10.1007/S40005-017-0361-5

Luo, C., Li, R., Tang, M., Gao, Y., Zhang, J., Qian, S., Wei, Y., & Shen, P. (2024). Amorphous solid dispersion to facilitate the delivery of poorly water-soluble drugs: recent advances on novel preparation processes and technology coupling. *Expert Opinion on Drug Delivery*. https://doi.org/10.1080/17425247.2024.2423813

Mansour, R. S. H., Deb, P. K., & Tekade, R. K. (2018). Role of Amorphous State in Drug Delivery. *Dosage Form Design Parameters*, *2*, 105–154. https://doi.org/10.1016/B978-0-12-814421-3.00004-X

Mehta, S. B., Shribak, M., & Oldenbourg, R. (2013). Polarized light imaging of birefringence and diattenuation at high resolution and high sensitivity. *Journal of Optics (2010)*, *15*(9), 10.1088/2040-8978/15/9/094007. https://doi.org/10.1088/2040-8978/15/9/094007

Meng, F., Ferreira, R., **Su, Y.** & Zhang, F. (2021). A novel amorphous solid dispersion based on drug–polymer complexation**.** *Drug Delivery and Translational Research*, **11**, 2072–2084. https://doi.org/10.1007/s13346-020-00869-3

Menczel, J. D., & Prime, R. B. (Eds.). (2009). *Thermal analysis of polymers: Fundamentals and applications*. John Wiley & Sons, Inc.

Moseson, D. E., Corum, I. D., Lust, A., Altman, K. J., Hiew, T. N., Eren, A., Nagy, Z. K., & Taylor, L. S. (2021). Amorphous Solid Dispersions Containing Residual Crystallinity: Competition Between Dissolution and Matrix Crystallization. *AAPS Journal*, *23*(4). https://doi.org/10.1208/S12248-021-00598-6

Moseson, D. E., Parker, A. S., Beaudoin, S. P., & Taylor, L. S. (2020). Amorphous solid dispersions containing residual crystallinity: Influence of seed properties and polymer adsorption on dissolution performance. *European Journal of Pharmaceutical Sciences*, *146*, 105276. https://doi.org/10.1016/J.EJPS.2020.105276

Newman, A., & Zografi, G. (2020). Commentary: Considerations in the Measurement of Glass Transition Temperatures of Pharmaceutical Amorphous Solids. *AAPS PharmSciTech*, *21*(1), 1–13. https://doi.org/10.1208/S12249-019-1562-1/FIGURES/13

Nunes, C., Mahendrasingam, A., & Suryanarayanan, R. (2006). Investigation of the multi-step dehydration reaction of theophylline monohydrate using 2-dimensional powder X-ray diffractometry. *Pharmaceutical Research*, *23*(10), 2393–2404. https://doi.org/10.1007/S11095-006-9022-5

Ojo, A. T., Ma, C., & Lee, P. I. (2020). Elucidating the effect of crystallization on drug release from amorphous solid dispersions in soluble and insoluble carriers. *International Journal of Pharmaceutics*, *591*, 120005. https://doi.org/10.1016/J.IJPHARM.2020.120005

Pandi, P., Bulusu, R., Kommineni, N., Khan, W., & Singh, M. (2020). Amorphous solid dispersions: An update for preparation, characterization, mechanism on bioavailability, stability, regulatory considerations and marketed products. *International Journal of Pharmaceutics*, *586*, 119560. https://doi.org/10.1016/J.IJPHARM.2020.119560

Perković, I., Poljak, T., Savijoki, K., Varmanen, P., Maravić-Vlahoviček, G., Beus, M., Kučević, A., Džajić, I. & Rajić, Z. (2023) 'Synthesis and Biological Evaluation of New Quinoline and Anthranilic Acid Derivatives as Potential Quorum Sensing Inhibitors', *Molecules*, **28**(15), 5866. https://doi.org/10.3390/molecules28155866.

Pereira, J., *et al.* Comparison of dissolution profiles: 90% confidence intervals of different f_2 estimators vs Euclidean distance. *Eur. J. Pharm. Sci.*, 2025.

Pöstges, F., Kayser, K., Stoyanov, E., & Wagner, K. G. (2022). Boost of solubility and supersaturation of celecoxib via synergistic interactions of methacrylic acid-ethyl acrylate copolymer (1:1) and hydroxypropyl cellulose in ternary amorphous solid dispersions. International Journal of Pharmaceutics: X, 4, 100115. https://doi.org/10.1016/J.IJPX.2022.100115

Raina, S. A., Alonzo, D. E., Zhang, G. G. Z., Gao, Y., & Taylor, L. S. (2014). Impact of polymers on the crystallization and phase transition kinetics of amorphous nifedipine during dissolution in aqueous media. *Molecular Pharmaceutics*, *11*(10), 3565–3576. https://doi.org/10.1021/MP500333V

Roudaut, G., Simatos, D., Champion, D., Contreras-Lopez, E., & Le Meste, M. (2004). Molecular mobility around the glass transition temperature: A mini review. *Innovative Food Science and Emerging Technologies*, *5*(2), 127–134. https://doi.org/10.1016/J.IFSET.2003.12.003

Rusdin, A., Mohd Gazzali, A., Ain Thomas, N., Megantara, S., Aulifa, D. L., Budiman, A., & Muchtaridi, M. (2024). Advancing Drug Delivery Paradigms: Polyvinyl Pyrolidone (PVP)-Based Amorphous Solid Dispersion for Enhanced Physicochemical Properties and Therapeutic Efficacy. *Polymers*, *16*(2), 286. https://doi.org/10.3390/POLYM16020286

S'Ari, M., Blade, H., Cosgrove, S., Drummond-Brydson, R., Hondow, N., Hughes, L. P., & Brown, A. (2021). Characterization of Amorphous Solid Dispersions and Identification of Low Levels of Crystallinity by Transmission Electron Microscopy. *Molecular Pharmaceutics*, *18*(5), 1905–1919. https://doi.org/10.1021/ACS.MOLPHARMACEUT.0C00918/SUPPL_FILE/MP0C00918_SI_001.ZIP

Savolainen, M., Kogermann, K., Heinz, A., Aaltonen, J., Peltonen, L., Strachan, C., & Yliruusi, J. (2009). Better understanding of dissolution behaviour of amorphous drugs by in situ solid-state analysis using Raman spectroscopy. *European Journal of Pharmaceutics and Biopharmaceutics : Official Journal of Arbeitsgemeinschaft Fur Pharmazeutische Verfahrenstechnik e.V*, *71*(1), 71–79. https://doi.org/10.1016/J.EJPB.2008.06.001

Schittny, A., Huwyler, J. & Puchkov, M. (2020). Mechanisms of increased bioavailability through amorphous solid dispersions: A review. Drug Delivery, 27(1), 110–127. https://doi.org/10.1080/10717544.2019.1704940

Skoog, D. A., Holler, F. J., & Crouch, S. R. (2017). *Principles of Instrumental Analysis* (7th ed.). Cengage Learning.

Strydom, S., Liebenberg, W., Yu, L., & de Villiers, M. (2009). The effect of temperature and moisture on the amorphous-to-crystalline transformation of stavudine. *International Journal of Pharmaceutics*, *379*(1), 72–81. https://doi.org/10.1016/J.IJPHARM.2009.06.012

Sun, Y., Zhu, L., Wu, T., Cai, T., Gunn, E. M., & Yu, L. (2012). Stability of Amorphous Pharmaceutical Solids: Crystal Growth Mechanisms and Effect of Polymer Additives. *The AAPS Journal*, *14*(3), 380. https://doi.org/10.1208/S12248-012-9345-6

Svoboda, R., Pakosta, M., & Doležel, P. (2023). How the Presence of Crystalline Phase Affects Structural Relaxation in Molecular Liquids: The Case of Amorphous Indomethacin. *International Journal of Molecular Sciences*, *24*(22), 16275. https://doi.org/10.3390/IJMS242216275/S1

Van den Mooter, G. (2014). The use of amorphous solid dispersions: A formulation strategy to overcome poor solubility and dissolution rate. *Drug Discovery Today: Technologies*, 9(2), e79–e85. https://doi.org/10.1016/j.ddtec.2011.10.002

Vasconcelos, T., Sarmento, B., & Costa, P. (2007). Solid dispersions as strategy to improve oral bioavailability of poorly water-soluble drugs. *Drug Discovery Today*, 12(23-24), 1068–1075. https://doi.org/10.1016/j.drudis.2007.09.005

Xue, Q., Lv, C., Shan, M., Zhang, H., Ling, C., Zhou, X., & Jiao, Z. (2013). Glass transition temperature of functionalized graphene-polymer composites. *Computational Materials Science*, *71*, 66–71. https://doi.org/10.1016/J.COMMATSCI.2013.01.009

Yao, X., Yu, L., & Zhang, G. G. Z. (2023). Impact of Crystal Nuclei on Dissolution of Amorphous Drugs. *Molecular Pharmaceutics*, *20*(3), 1796–1805. https://doi.org/10.1021/ACS.MOLPHARMACEUT.2C00989

Zelkó, R., & Szakonyi, G. (2012). The effect of water on the solid state characteristics of pharmaceutical excipients: Molecular mechanisms, measurement techniques, and quality aspects of final dosage form. *International Journal of Pharmaceutical Investigation*, *2*(1), 18. https://doi.org/10.4103/2230-973X.96922

Zhang, J., Guo, M., Luo, M., & Cai, T. (2023). Advances in the development of amorphous solid dispersions: The role of polymeric carriers. *Asian Journal of Pharmaceutical Sciences*, *18*(4), 100834. https://doi.org/10.1016/J.AJPS.2023.100834

Zografi, G., & Newman, A. (2017). Interrelationships Between Structure and the Properties of Amorphous Solids of Pharmaceutical Interest. *Journal of Pharmaceutical Sciences*, *106*(1), 5–27. https://doi.org/10.1016/J.XPHS.2016.05.001

Chapter 4

Conclusion and Recommendations

4.1.1 Study Outcome and Conclusions

Improving drug solubility and bioavailability remains a significant focus in pharmaceutical development, particularly for poorly water-soluble compounds (Bhujbal et al., 2021; Schittny et al., 2020). The studied chloroquinoline-urea-benzothiazole compound demonstrated initial poor aqueous solubility, which posed considerable formulation challenges. However, the development of an ASD using PVP K25 markedly enhanced its solubility relative to the raw material, achieving concentrations up to 19.399 µg/mL in water. This contrasted sharply with the negligible solubility exhibited by the unformulated raw material, emphasizing the efficacy of the ASD approach. In addition, dissolution studies showcased potential for further improvements to these characteristics in the ASD and further enhancements to its profile as well as potential extension of studies to more robust models (Rusdin et al., 2024).

Stability analysis pointed to a significant advantage in terms of the thermal stability of the ASD (Hancock & Zografi, 1997; Lehmkemper et al., 2017). The high *T*g observed suggests that the prepared ASD maintains thermal integrity under a range of conditions, indicating potential long-term stability however its unsatisfactory results during XRPD studies, with slight crystallinity detected, suggests that strong emphasis on formulation technique needs to be employed to potentially remove this flaw in the formulation and in essence increase its solubility and stability performance (Bhujbal et al., 2021). More in-depth polymer selection studies may be conducted to look more closely at the compound's versatility in formulation.

4.2.1 Recommendations for Future Studies

- Further exploration of solvent systems that avoid the limitations seen with DCM, aiming for complete amorphicity in the final product, should be conducted to enhance formulation performance (Bhujbal et al., 2021).
- Exploration in technique alteration to non-solvent based ones such as quench cooling, hot melt extrusion or cryogenic ball milling to assess effect of technique selection (Bhujbal et al., 2021).
- Investigation into temperature-controlled X-ray diffraction for the ASD to further examine potential new crystalline solid-state forms for the compound (Karjalainen et al., 2005; Kumar et al., 2020).

- Additional studies on *in vivo* bioavailability to confirm the enhanced solubility benefits observed *in vitro* are recommended (Schittny et al., 2020).
- Investigation into alternative polymer carriers such as polyethylene glycol, Eudragit® series, HPMC or copovidone and combinations that might offer improved dispersion characteristics and potentially higher solubility outcomes (Nair et al., 2020; Corrie et al., 2023).
- A broader analysis involving stability testing under different storage conditions such as increased humidity to validate the high *T*g findings and assess real-world stability as well as rate of crystallisation (Hancock & Zografi, 1997; Lehmkemper et al., 2017).
- More reliable ways to obtain the raw material would need to be explored in future. A possible ways to circumvent this issue would be to synthesise the required chloroquinoline derivative on-site en masse.
- Follow up studies to look at the effects of extended heat parameters beyond *T*m on the characteristics of the raw material and ASD as well as VT-XRPD and hot stage microscopy to further separate the overlapping processes within the DSC to also be considered for future (Karjalainen et al., 2005; Kumar et al., 2020).

Reference List

Bhujbal, S. V., Mitra, B., Jain, U., Gong, Y., Agrawal, A., Karki, S., Taylor, L., Kumar, S., & Zhou, Q. (2021). Pharmaceutical amorphous solid dispersion: A review of manufacturing strategies. Acta Pharmaceutica Sinica B. https://doi.org/10.1016/j.apsb.2021.05.014

Corrie, L., Ajjarapu, S., Banda, S., Parvathaneni, M., Bolla, P. K., & Kommineni, N. (2023). HPMCAS-based amorphous solid dispersions in clinic: A review on manufacturing techniques (hot-melt extrusion and spray drying), marketed products and patents. Materials, 16(20), 6616. https://doi.org/10.3390/ma16206616

Hancock, B. C., & Zografi, G. (1997). The relationship between the glass transition temperature and the water content of amorphous pharmaceutical solids. Pharmaceutical Research, 11(4), 471–477. https://doi.org/10.1023/A:1018941810744

Karjalainen, M., Airaksinen, S., Rantanen, J., Aaltonen, J., & Yliruusi, J. (2005). Characterization of polymorphic solid-state changes using variable temperature X-ray powder diffraction. Journal of Pharmaceutical and Biomedical Analysis, 39(1–2), 273–279. https://doi.org/10.1016/j.jpba.2005.02.036

Kumar, A., Singh, P., & Nanda, A. (2020). Hot stage microscopy and its applications in pharmaceutical characterization. Applied Microscopy, 50, 7. https://doi.org/10.1186/s42649-020-00032-9

Lehmkemper, K., Kyerematen, S. O., Heinzerling, O., Degenhardt, M., & Sadowski, G. (2017). Impact of polymer type and relative humidity on the long-term physical stability of amorphous solid dispersions. Molecular Pharmaceutics, 14(12), 4374–4386. https://doi.org/10.1021/acs.molpharmaceut.7b00637

Nair, A. R., Lakshman, Y. D., Anand, V. S. K., Sree, K. S. N., Bhat, K., & Dengale, S. J. (2020). Overview of extensively employed polymeric carriers in solid dispersion technology. AAPS PharmSciTech, 21, 309. https://doi.org/10.1208/s12249-020-01849-z

Rusdin, A., Gazzali, A. M., Thomas, N. A., Megantara, S., Aulifa, D. L., Budiman, A., & Muchtaridi, M. (2024). Advancing drug delivery paradigms: Polyvinylpyrrolidone (PVP)-based amorphous solid dispersion for enhanced physicochemical properties and therapeutic efficacy. Polymers, 16(2), 286. https://doi.org/10.3390/polym16020286

Schittny, A., Huwyler, J., & Puchkov, M. (2020). Mechanisms of increased bioavailability through amorphous solid dispersions. Drug Delivery, 27(1), 110–127. https://doi.org/10.1080/10717544.2019.1704940

Appendices

Appendix 1: FTIR Spectral Analysis of the chloroquinoline derivative and its Amorphous Solid Dispersion

Aim: To analyse the Fourier Transform Infrared (FTIR) spectra of the raw the chloroquinoline derivative and its amorphous solid dispersion to identify characteristic functional groups and possible molecular interactions.

Method: FTIR spectra were obtained for both the raw chloroquinoline derivative and the amorphous solid dispersion using an FTIR spectrometer. The wavenumber range was set from 4000 to 400 cm^{-1}, and the resolution was maintained at 4 cm^{-1}.

Results:

The spectra for the raw chloroquinoline derivative showed distinct peaks corresponding to its crystalline structure.

The spectra for the ASD demonstrated shifts in specific absorption bands, indicating interactions between the chloroquinoline derivative and PVP K25 polymer, which suggest successful formulation of the amorphous state.

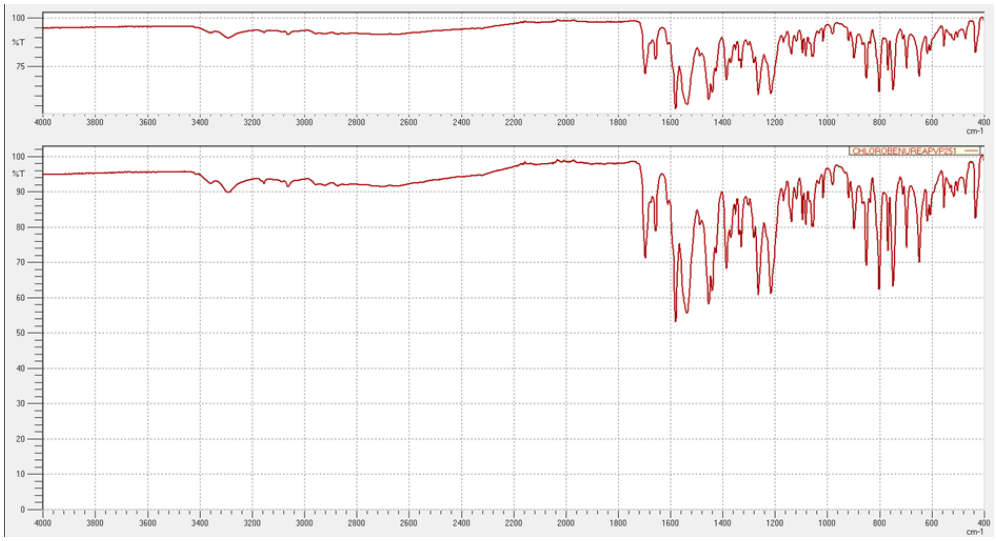

Figure A1: FTIR spectra of PVP-K25

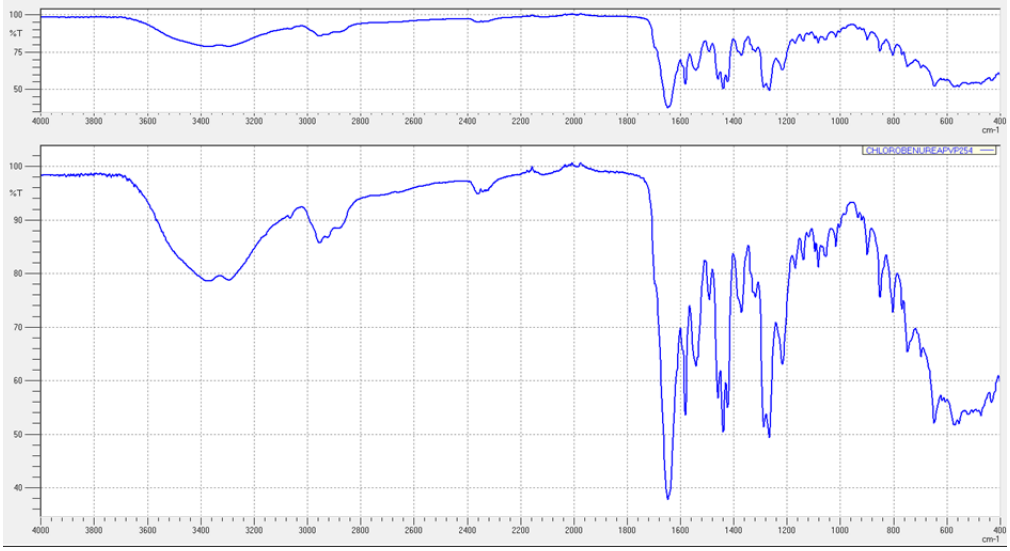

Figure A2: FTIR spectra of 1:4 physical mixture